ORIGINAL RESEARCH PAPER

Chemistry

VIBRATIONAL ANALYSES OF ALKALOID COCAINE AS FREE BASE, CATIONIC AND HYDROCHLORIDE SPECIES BASED ON THEIR INTERNAL COORDINATES AND FORCE FIELDS

KEY WORDS: Cocaine, vibrational spectra, molecular structure, descriptor properties, DFT calculations

Davide Romani SST, Servicio sanitario della Toscana, Azienda USL 9 di Grosseto

Silvia Antonia Brandán Cátedra de Química General, Instituto de Química Inorgánica, Facultad de Bioquímica. Química y Farmacia, Universidad Nacional de Tucumán

ABSTRACT

The structural, electronic, topological and vibrational properties of the free base, cationic and hydrochloride species of cocaine in gas and aqueous solution phases have been studied from theoretical point of view by using hybrid calculations derived from the density functional theory (DFT). The experimental available ATR, FTIR, FTRaman and Terahertz spectra for the free base and the hydrochloride species, the corresponding normal internal coordinates together with the scaled quantum mechanical force field (SQMFF) approach were employed in order to perform the complete vibrational assignments of those three species of cocaine. The NBO and AIM calculations support the high stabilities observed for the cationic species while their higher gap energy could justify their low reactivities in both media. The O--O interactions predicted by AIM analysis for the hydrochloride species in both media could support the high reactivities of this species in both media, as suggested by their gap energy values. All properties and the force fields were calculated at the B3LYP/6-31G* level of theory. The force constants and the complete assignments of the 123, 126 and 129 vibration normal modes expected for the free base, cationic and hydrochloride species respectively are reported for first time. In addition, the predicted IR spectrum for cocaine hydrochloride reveals that in the solid state this species is in their cationic form, as observed by the experimental IR spectrum. The cation cocaine in both media is most electrophilic and reactive than the cation tropane increasing notably their reactivity. However, the nucheophilicity indexes for the tropane alkaloid in both media are comparable to those observed for toxics substances as saxitoxin and cation pyridonium. Probably these results for tropane, different from cocaine species, suggest that the modifications in the stereochemistry of tropane generate a loss in their potency, as was reported in the literature

INTRODUCTION

Cocaine is a drug of abuse broadly known and studied from different points of view [1-16], being their IUPAC name, Methyl (3S)-3-(benzoyloxy)-8-methyl-8-azabicyclo[3.2.1]octane-2-carboxylate. The structures of this alkaloid as free base and as hydrochloride were already reported by Hrynchuk et al. [2] and Gabe and Barnes, respectively [1]. The pharmacological and medicinal properties that have these tropyl alkaloids are attributed to the tertiary nitrogen atom belonging to the >N-CH_3 group, as reported in the literature [17-28]. The identification of this drug in all media is of interest, in general for the forensic science in order to avoid their adulteration and abuse, and, in particular for the human health because their use is strongly associated with bronchiolitis obliterans organizing pneumonia [3] and with elicits autophagic cytotoxicity via a nitricoxide, as was recently reported that high doses of cocaine cause your brain cells to kill themselves [16]. Vibrational spectroscopy is the technique most used to identify cocaine because it is no destructive, quick, and with few quantity of sample the infrared and Raman spectra can be easily recorded [5,10,11-15]. Thus, the Horizontal Attenuated Total Reflectance (HATR), FT-IR and FT-Raman spectra were used by different authors to quantify mixed of cocaine based on the principal component regression (PCR) [5,29] or simply to identify it using a fast screening method [30,31]. In some cases, the main functional groups of cocaine were identified but, so far, the complete assignments of their vibrational spectra were not reported. Probably, the presence in all tropane alkaloids of a bicyclic (N-methyl-8-a-zabicyclo[3.2.10]octane) structure constituted by two fused piperidine and pyrrolidine rings is the major difficult to assign all bands observed in their corresponding vibrational spectra. At the moment, taking into account that the normal internal coordinates were recently elucidated for the alkaloid tropane [32] it is possible to perform the complete vibrational analyses of the three cocaine forms, as free base, cationic and hydrochloride, based on their force fields and by using the SQM methodology. Such studies are important because, as reported by Lazny et al. [33], the tropane derivatives at room and low temperature undergo fast N-methyl inversion in aqueous and methanol solutions. Hence, the aims of this work are: (i) to optimize the three cocaine structures, as free base, cationic and hydrochloride by using the hybrid B3LYP/6-31G* method [34,35] in gas and aqueous solution phases in order to observe if some of these species present N-methyl inversion in solution, (ii) to perform the complete vibrational analyses of these three species by using their experimental available infrared and Raman spectra, their normal internal coordinates and their corresponding force fields and finally, (iii) to compare their structural and electronic properties and force constants with those reported for the tropane alkaloid in both media. The predictions of the reactivities and behaviours of those three species in both media are of interest due to that all tropane alkaloids present anticholinergic activities, as suggested by Pauling and Datta [36], for these reasons, the frontier orbitals [37,38] and some descriptors were also calculated for those three species [39-41].

COMPUTATIONAL INFORMATION

The GaussView program [42] was used to model the cocaine structures as free base, cationic and hydrochloride in accordance to those experimental structures reported for the free base and hydrochloride forms [1,2]. Later, these structures were optimized by using hybrid B3LYP/6-31G* calculations with the Gaussian 09 program [43]. In all structures, the piperidine rings were optimized in their most stable chair structure, as was experimentally observed for cocaine as free base and hydrochloride species [1,2] and also, in some tropane alkaloids [44-47]. **Figure 1** shows the theoretical structures of cocaine as free base, cationic and hydrochloride and the atoms numbering while, in **Figure 2** are observed these structures with the identifications of their three rings, which are, one benzyl and the fused piperidine and pyrrolidine rings belonging to the (N-methyl-8-a-zabicyclo[3.2.10]octane) systems.

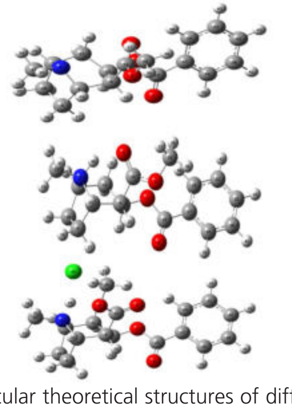

Figure 1. Molecular theoretical structures of different species of alkaloid cocaine: a) free base, b) cationic and, c) hydrochloride and the atoms numbering.

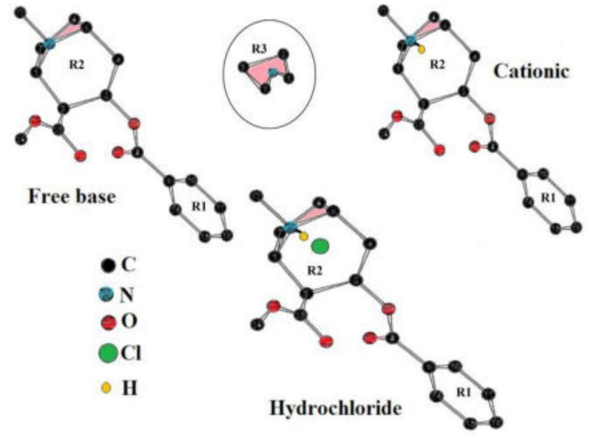

Figure 2. Perspective view of the molecule of cocaine in accordance to the experimental structure reported for the hydrochloride cocaine [1] with the atoms numbering and the identifications of the benzyl, piperidine and pyrrolidine rings.

Here, R1 correspond to the benzyl ring while R2 and R3 match to the piperidine and pyrrolidine rings, respectively. In solution, the calculations were performed at the same level of theory by using the self-consistent reaction field (SCRF) method with the integral equation formalism variant polarised continuum (IEFPCM) model [48,49] because both methods consider the solvent effects. On the other hand, the solvation energies for the three species were calculated with the solvation model [50], as implemented in the Gaussian program [43] while the volume variations in solution were computed with the Moldraw program [51] by using the same method. Additionally, the SQMFF procedure [52] together with the Molvib program [53] was employed to calculate the force fields for the three species. At this point, the normal internal coordinates corresponding to the tropane ring of the three species of cocaine were taken from those built for the alkaloid tropane [32] while the remaining coordinates for the benzyl ring and COO groups are similar to those reported for compounds containing these groups [40,41]. In this work, the atomic natural population (NPA) and the Merz-Kollman (MK) charges [54] were studied for the three species together with their topological properties. Hence, the natural bond orbital (NBO) and AIM2000 programs were also used to obtain the bond orders and the stabilization energies based on the main donor-acceptor energy interactions. Afterwards, the force fields were calculated for those three cocaine species in both media by using the B3LYP/6-31G* method, the SQMFF methodology [52] and the Molvib program [53]. The complete vibrational assignments were performed taking into account the Potential Energy Distribution (PED) 10%. The force constants for the free base, cationic and hydrochloride species of cocaine in both media were also calculated after to transform their force fields obtained in cartesian coordinates to normal internal coordinates. The HOMO-LUMO orbitals [37,38] and some known descriptors were also calculated for those three species [39-41] due to the recognized activities that present the alkaloid cocaine.

RESULTS AND DISCUSSION

Studies in gas phase and solution

Table 1 shows the total energies, dipole moments, volume variation and solvation energy for the free base, cationic and hydrochloride cocaine species calculated in gas and aqueous solution phases by using the hybrid B3LYP/6-31G* level of theory. Analyzing carefully the dipole moment values we observed that the cationic species present the higher values in both media, as can be seen in **Figure S1.**

TABLE – 1

Calculated total energies (E), dipole moments (μ), volume variations (ΔV) and solvation energies (ΔG) for the free base, cationic and hydrochloride cocaine species in gas and aqueous solution phases.

B3LYP/6-31G*				
Gas phase				
Species	E (Hartrees)	μ (D)	V (Ĺ3)	
Free base	-1016.1192	1.55	321.0	
Cation	-1016.5254	9.57	322.5	
H-Cl	-1476.9360	7.45	353.2	
PCM				
	E (Hartrees)	μ (D)	V (Å3)	ΔV (Å3)
Free base	-1016.1351	1.86	322.2	1.2
Cation	-1016.6092	13.22	323.7	1.2
H-Cl	-1476.9758	12.58	352.5	-0.7
Solvation energy (kJ/mol)				
	$\Delta G_u^{\#}$	ΔG_{ne}	ΔG_c	
Free base	-41.70	28.51	-70.21	
Cation	-219.81	38.58	-258.39	
H-Cl	-104.39	38.20	-142.59	

Hence, the magnitudes and orientations of the corresponding vectors are completely different in the three species. Note that the cationic form is probably the most hydrated species in solution because it is a charged species. In relation to the volumes, the hydrochloride species present the higher values in both media where the free base and the cationic species show higher expansions in solution while a volume contraction is observed for the hydrochloride species. Here, the volume variations were calculated from the differences between the values in solution in relation to the values in gas phase with the Moldraw program [51]. On the other hand, the higher solvation energy is also observed for the cationic form, as expected due to their higher hydration. The solvation energy corrected values were calculated taking into account the total non electrostatic terms due to the cavitation, dispersion and repulsion energies, as calculated from the SMD model [50]. These results are in agreement with those observed for the tropane species where the hydrochloride form also present the higher volume variations due to the presence of the Cl atom in their structure [32]. From the same way, the free base of cocaine also presents the lower solvation energy values, as compared with the corresponding tropane species, in correlation with their low dipole moment values in both media. Table 1 shows a slightly increase of the dipole moment values for all the species in solution, as a consequence of their hydrations.

Structural study in gas phase and in aqueous solution

In **Table 2** are summarized the theoretical geometrical parameters calculated for the free base, cationic and hydrochloride cocaine species in gas and aqueous solution phases compared with that experimental structure observed for cocaine hydrochloride in the solid phase by Gabe and Barnes [1] and with that experimental observed for the free base by Hrynchuk et al. [2]. The comparisons were performed by using the root mean square deviation (RMSD) values. When all calculated bond lengths in gas phase are represented for each species in **Figure 2Sa** as a function of the experimental hydrochloride values we observed little variations in all parameters but, when the C-O and N-C distances are graphed for the three species in **Figure 2Sb** and **2Sc** slightly variations in the C15=O4, N5-C6 and N5-C7 distances are observed. Here, the higher variation observed in the RMSD values for the hydrochloride species in the gas phase from 0.030 Ĺ to 0.800 Ĺ in solution can be attributed to their volume contraction in this media, as observed in Table 1 because some bond lengths and angles decrease their values in solution. Regarding the bond angles calculated for the free base, cationic and hydrochloride cocaine species in gas phase at the B3LYP/6-31G* level of theory we observed significant variations for some angles in relation to the experimental ones, as observed in **Figure S3**. Thus, Figure S3a shows clearly that the C13-N5-C6 and C13-N5-C7 angles are practically the same in the three species but slightly different from the experimental ones while the free base presents the N5-C6-C9, N5-C7-C10 and C6-C9-C10 angles different from the other two species including the experimental ones. On the other hand, Figure 3Sb shows the differences in the dihedral angles where, the C8-C6-N5-C13 and O4-C15-O1-C12 angles have the same values in the three species but, in the hydrochloride species the C8-C14-O2-C16 angle is different from the observed in the other two species while the C17-C15-O1-C12 angle is different only in the cationic species. When the calculated dihedral C11-C12-O1-C15 angles for all species are compared with those observed for the two experimental structures the better correlation in both media are obtained for the free base, as expected because for hydrochloride the experimental angles are -73/-77 ş.

Charges, molecular electrostatic potentials and bond orders studies

For the three cocaine species in both media, the MK and NPA charges together with the molecular electrostatic potentials were studied by using B3LYP/6-31G* calculations. The results can be seen in **Tables S1** and **S2** (Supporting material). There are notable differences between both charges on the O and N atoms corresponding to the three species, as observed in **Figure S4**.

TABLE – 2 Comparison of calculated geometrical parameters for the free base, cationic and hydrochloride cocaine species in gas and aqueous solution phases compared with the corresponding experimental ones for free base and hydrochloride cocaine.

Parameters	B3LYP/6-31G*[a]						Exp[b]	Exp[c]
	Free base		Cationic		Hydrochloride			
	Gas	PCM	Gas	PCM	Gas	PCM		
Bond lengths (Å)								
N5-CH_3	1.459	1.467	1.493	1.492	1.487	1.494	1.478	1.468
N5-C6	1.475	1.479	1.527	1.521	1.511	1.519	1.487	1.467
N5-C7	1.478	1.485	1.525	1.522	1.512	1.520	1.503	1.460
C6-C9(A5)	1.561	1.556	1.543	1.542	1.550	1.545	1.525	1.522
C7-C10(A5)	1.562	1.556	1.544	1.540	1.544	1.542	1.562	1.527
C6-C8(A6)	1.555	1.557	1.546	1.545	1.543	1.549	1.544	1.532
C7-C11(A6)	1.541	1.540	1.535	1.533	1.536	1.536	1.544	1.531
C8-C12(A6)	1.540	1.540	1.561	1.557	1.559	1.549	1.524	1.511
C11-C12(A6)	1.532	1.529	1.534	1.530	1.531	1.530	1.558	1.518
C12-O1	1.447	1.454	1.425	1.445	1.429	1.443	1.385	1.451
C15=O4	1.219	1.225	1.213	1.222	1.218	1.224	1.172	1.193
C14-O2	1.355	1.347	1.318	1.330	1.346	1.343	1.291	1.334
C14=O3	1.210	1.220	1.229	1.226	1.208	1.217	1.250	1.188
O2-CH_3	1.437	1.445	1.453	1.450	1.445	1.446	1.432	1.442
RMSD[b]	**0.033**	**0.032**	**0.027**	**0.030**	**0.030**	**0.800**		
RMSD[c]	**0.022**	**0.022**	**0.033**	**0.030**	**0.027**	**0.800**		
Bond angles (º)								
C13-N5-C6	113.8	112.1	114.5	114.1	114.0	113.2	112.5	112.7
C13-N5-C7	113.9	112.4	114.8	114.5	114.3	113.8	112.4	113.2
C6-N5-C7(A5,A6)	101.7	101.1	101.5	101.8	101.8	101.7	103.6	100.9
N5-C6-C9(A5)	105.3	105.6	102.8	102.6	102.5	102.0	102.3	105.4
N5-C7-C10(A5)	105.0	105.2	102.4	102.4	102.9	102.3	101.1	106.2
C6-C9-C10(A5)	103.7	103.7	105.1	105.1	105.0	105.2	105.8	103.8
N5-C6-C8(A6)	106.9	107.6	107.1	107.9	108.9	109.0	108.0	106.8
N5-C7-C11(A6)	107.3	107.6	107.1	106.9	106.6	107.2	109.1	106.7
C8-C12-C11(A6)	112.4	113.0	112.2	112.9	112.4	112.3	112.8	112.2
RMSD[b]	**2.1**	**2.1**	**1.6**	**1.4**	**1.5**	**1.2**		
RMSD[c]	**0.7**	**0.7**	**1.8**	**1.8**	**1.8**	**2.0**		
Dihedral angles (º)								
C8-C6-N5-CH_3(A6)	-160.1	-163.8	-160.7	-161.8	-161.9	-164.3		
C11-C12-O1-C15	-151.0	-147.3	-157.1	-153.7	-162.2	-156.3	-73-77	-139
C8-C14-O2-C16	179.7	-178.0	176.8	177.8	-175.8	177.6		
C17-C15-O1-C12	-177.3	-179.0	177.3	179.4	-176.5	-177.6		
O4-C15-O1-C12	3.0	1.3	-2.6	-0.4	4.3	2.4		

[a]This work, [b]Ref [1] for hydrochloride cocaine; [c]Ref [2] for free base cocaine; A6, six member's ring (piperidine); A5, five member's ring (pyrrolidine).

Thus, the behaviours of the MK charges on the O and N atoms are negative and practically similar for the free base and the cationic species but, for the hydrochloride the MK charge on the N atom change to a positive value. Note that the higher MK charges are observed in all species on the O3 atoms. Analyzing the NPA charges from Figure S4 we observed that these charges on the O and N atoms corresponding to the free base and the hydrochloride species are similar but, for the cationic species, the NPA charge on the O2 is less negative than the other ones while the charges on the O3 atom is most negative than the other ones. On the other hand, the NPA charges on the N atoms of the three species present practically similar values. When the MK charges on the C atoms corresponding to the pyrrolidine and piperidine rings are graphed for the three species in **Figure S5** we can observe some interesting differences. The behaviours of the MK charges on the C atoms in the two rings are similar for the free base and the cationic species while for the hydrochloride species the values on the C6, C7 and C8 atoms change notably, having in the two first cases lower values while in the other ones higher values, as observed in Figure S5. Evidently, the presence of the electronegative Cl atom in the hydrochloride species has influence on their properties.

The molecular electrostatic potential (MEP) values for all atoms of the three species are presented in Table S1. These values are strongly related to the MK charges because they are calculated by using these charges. The most negative values are observed on the Cl atoms, as expected due to their higher electronegativity and, there are not significant differences in the values showing in all species the following tendency: Cl > O > N > C >H. In reference to the O atoms, the higher MEP values are observed on the O3 atoms of the free base and the hydrochloride species and on the O4 atoms of the cationic species in both media. However, when the mapped MEP surfaces are obtained we observed differences in the regions nucleophilic and electrophilic thought their red and blue colorations, respectively. Thus, **Figure S6** shows strong red colour on the O atoms corresponding to the COO groups of the free base while in the cationic species is completely observed a blue colour, as expected because it is an electrophilic species. On the contrary, in the hydrochloride species we observed red colour on the Cl atom and COO groups and blue colour on the tropane rings. Note that in the cationic and hydrochloride species the less negative values are observed on the H44 atoms in both media because they are the most labile atoms. For these reasons, in the MEP mapped of those two species we observed the strong blue colour on those H atoms.

In relation to the bond orders (BO), in Table S2 are summarized these results for all cocaine species, expressed as Wiberg indexes. The results show some differences in the values for the C atoms corresponding to the piperidine and pyrrolidine rings, as observed in **Figure S7**. This way, the free base presents the higher BO values while in the cationic species it is observed the lower values. Note that in all species the C8 atoms corresponding to the piperidine rings have the higher BO values.

Stability studies by NBO and AIM calculations

From the above studies we observed that the three species present different properties and, for these reasons, we have studied the stabilities of those species by using NBO and AIM calculations [55,56]. In **Table S3** are summarized the results of the donor-acceptor energy interactions for the free base, cationic and hydrochloride structures of cocaine by using the hybrid B3LYP/6-31G* level of theory. It is necessary to clarify that these values were obtained from the second order perturbation theory analysis of Fock matrix with the NBO calculations [55]. First, we observed common interactions to the three species, which are the π*O4-C15π*C17-C19, ΔET_{*} and ΔET_{LP*} interactions and, then, only those observed in the cationic (π*C17-C19π*C18-C20 and LP(2)O3 σ*N5-C14) and in the hydrochloride species ($\Delta ET_{\sigma\rightarrow LP*}$ and $\Delta ET_{LP\rightarrow LP*}$). These additional interactions confer high stabilities to both cationic and hydrochloride species being their total energy values of 2682.60 and 3727.43 kJ/mol, respectively. This NBO study shows clearly that the species most unstable in both media is the free base while both, cationic and hydrochloride species are the most stable in those media.

In relation to the AIM study [56], the topological properties were calculated for all the species in order to investigate the possible intra-molecular interactions existent in these species in both media. Here, the results obtained from the atoms in molecules (AIM) analyses are observed for the free base and cationic species in **Table S4** while in **Table S5** are presented the results for the hydrochloride species. According to the Bader's theory [57] it is necessary to calculate the following parameters: electron density, ρ(r), the Laplacian values, $\nabla^2\rho(r)$, the eigenvalues ($\lambda1, \lambda2, \lambda3$) of the Hessian matrix and, the $|\lambda1|/\lambda3$ ratio calculated in the bond critical points (BCPs) because their values show clearly the interaction's types. Thus, the H bonds formation is observed when $|\lambda1|/\lambda3 < 1$ and $\nabla^2\rho(r) > 0$ [58]. Besides, these parameters can be computed in the ring critical points (RCPs) of the benzyl, piperidine and pyrrolidine rings and, in the new rings formed as a consequence of the H bonds constituted (RCPN). Here, for the free base in both media, it is observed one H bonds, named O3---H31 while, for the cationic species we observed the O3---H44 interaction in gas phase while in solution appear two O3---H44 and C19---H38 interactions that probably explain their higher hydration, it is the higher solvation energy and their higher dipole moment value. The hydrochloride species also shows differences in both media, thus, in gas phase present four H bonds while in solution only three interactions are observed. Hence, the hydrochloride species is the most stable species but, in particular, the O3---O1 interactions observed in the two media could explain the diminishing of their stabilities as a consequence of the strong repulsion between those two electronegative atoms due to the 2.750-2.755 Ĺ distance values. **Figure S8** shows the molecular graphics for the free base, cationic and hydrochloride cocaine species in gas phase showing the geometry of all their bond critical points (BCPs) and ring critical points (RCPs) at the B3LYP/6-31G* level of theory. On the other hand, the analyses of the densities of the three different benzyl, piperidine and pyrrolidine rings, named RCP1, RCP2 and RCP3, respectively show that the piperidine rings have the lower values in the three species while the higher values are observed in the pyrrolidine rings corresponding to the three species, having the free base the higher value. These results are probably related with the strong blue coloration observed in all the species on the piperidine rings corresponding to the tropane rings.

HOMO-LUMO and descriptors studies

Pauling and Datta [36] have suggested that all tropane alkaloids can present anticholinergic activities and, for this reason, it is interesting to calculated the highest occupied molecular orbital (HOMO) and the lowest unoccupied molecular orbital (LUMO) in order to predict the reactivities and behaviours of the free base, cationic and hydrochloride species of cocaine in both media. Thus, the differences energies between those two orbitals, named gap energy [37,38], were calculated for all species together with recognized descriptors [39-41] whose known equations are presented in the same table. The values can be seen in **Table S6** together with some values for the three species of tropane alkaloid calculated in this work and, with other reported in the literature for antiviral agents, as cidofovir and brincidofovir [59], with antimicrobial 1,3-benzothiazole, as thione and thiol [60] and with toxic agents, as saxitoxin and cation pyridonium [39]. Analyzing first the gap values among the three species of cocaine we observed that the hydrochloride species is the most reactive in both media while the cationic species is the less reactive contrarily to the expected. Another very important result is that in solution the hydrochlorides species decrease notably their reactivity probably because, as observed from the NBO and AIM results, increase their stability in solution. When the values are compared with those calculated for the three tropane species we observed that also the hydrochloride species is the most reactive in both media while the cationic species is the less reactive but, the incorporation of COO groups and the benzyl ring in cocaine increase notably the reactivities of all their species, as compared with the tropane ones. These results could probably explain the strong biological activities that present cocaine. Note that the gap energy in solution for the hydrochloride species of cocaine is comparable to those observed for thione and brincidofovir [59,60] while are for the free base and the cationic species the gap values are lower that those observed for saxitoxin and cation pyridonium [39]. Comparing the descriptors for the cocaine species we observed that, as expected, the most electrophilic species is the cationic but, the cation tropane is twice most nucleophilic than the corresponding to cocaine being, the cation cocaine most nucleophilic than the other ones. These results could be in agreement with those observed by Singh [61] in a study on cocaine antagonists, where this author has observed that modifications in the stereochemistry of tropane led to a significant loss in their potency. Another important result is that the electrophilic indexes for saxitoxin and cation pyridonium [39] are similar to those observed for the cation tropane because they also are structurally cations. The behaviours of all descriptors in both media can be easily seen in **Figure S9** where clearly it is observed the most negative energies for the cationic species of cocaine. All the tropane species have the same behaviours than the corresponding to cocaine and, for these reasons, the graphics in both media are not presented here. These results suggest that the hydrochloride species in solution are as cationic species for which are most stable and have lower reactivity in both media.

VIBRATIONAL ANALYSIS

This analysis was performed with the optimized C_1 structures for the free base, cationic and hydrochloride species of cocaine in both media by using the hybrid B3LYP/6-31G* method. These calculations predicted 123, 126 and 129 vibration normal modes for the free base, cationic and hydrochloride species, respectively and, due to their symmetries; all vibration modes can present activities in the infrared and Raman spectra. Here, the infrared and Raman spectra for the free base and the hydrochloride species were taken from those reported in the literature [12,14,31,62]. The Raman spectra for those two cocaine species in the solid states were taken from those spectra published by Ryder et al. [5] and

Fedchak [63]. The terahertz spectrum of cocaine reported by Davies et al [9] was used to obtain the bands observed in the lower wavenumbers region. The comparisons among the predicted infrared spectra for the free base, cationic and hydrochloride species with the experimental available for the free base and hydrochloride species are observed in **Figure 3** while in **Figures 4** and **5** are presented the comparisons among the Raman spectra.

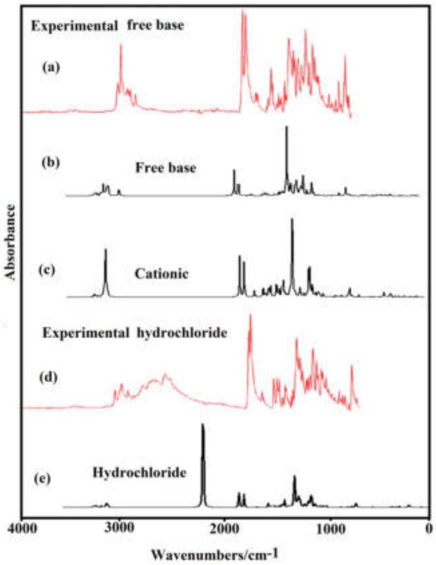

Figure 3. Comparisons between the experimental available FTIR spectra of free base and hydrochloride species of cocaine in the solid states [12,14,31] with the corresponding predicted for the free base, cationic and hydrochloride species in the gas phase at B3LYP/6-31G** level of theory.

Figure 3 clearly evidence that in the solid phase the hydrochloride species is present as cationic because the strong band predicted for this specie by calculations is not observed in the experimental IR spectrum. Here, obviously in the theoretical spectra we not observed broad bands because the calculations are performed in the gas phase for the isolated molecules while in the solid phase the forces packing are important. In Table 3 are given the observed and calculated wavenumbers for the free base, cationic and hydrochloride species of cocaine in gas phase and their corresponding assignments. Here, the predicted Raman spectra for the three cocaine species show a very good concordance when their activities are transformed to intensities by using known equations [64,65]. The normal internal coordinates for all species were used together with the SQMFF methodology [52] and the Molvib program [53] to calculate the force fields. The scale factors reported by Rauhut and Pulay [52] valid for the 6-31G* basis set were used to obtain the scaled force fields while the complete assignments were performed using the potential energy distribution (PED) contributions 10 %. It is necessary to clarify that in the higher wavenumbers region was not possible to identify the symmetries of the vibration normal modes because the experimental available Raman spectrum only was reported from 2000 cm^{-1}.

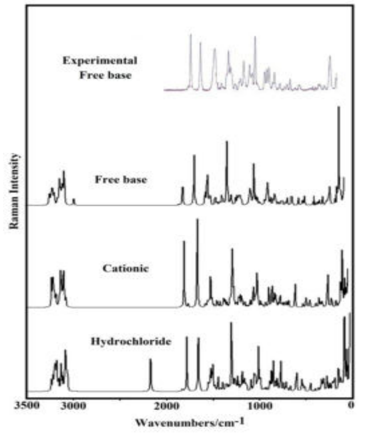

Figure 4. Comparisons between the experimental available Raman spectra of free base and hydrochloride species of cocaine in the solid states [5,63] with the corresponding predicted for the free base, cationic and hydrochloride species in the gas phase at B3LYP/6-31G** level of theory.

Here, the assignments performed for the most important groups are discussed briefly at continuation.

Band Assignments

NH modes. These vibration modes are predicted only for the cationic and hydrochloride species because the free base does not present this group. In the cationic species of tropane, the N-H stretching mode is assigned at 3419 cm^{-1} while for the hydrochloride species is assigned at 1626 cm^{-1}. In clonidine hydrochloride is assigned to 3427 cm^{-1} while in their monomer neutral at 1711 cm^{-1} [66], in tricyclic bisguanidine species these modes appear between 3403 and 3397 cm^{-1} [39] while in other compounds these stretching modes are assigned between 3480 and 3254 cm^{-1} [68-70]. Here, the cationic species is predicted by SQM calculations at 2989 cm^{-1} while in the hydrochloride at 2089cm^{-1}. Hence, the shoulders at 2982/2981 cm^{-1} can be assigned to these modes for the cationic species while the strong ATR band in the hydrochloride spectrum at 2545 cm^{-1} is assigned to the N-H stretching modes. In the cationic and hydrochloride species of tropane, the out-of-plane deformation modes are assigned between 1626 and 1393 cm^{-1} because they are predicted between 1532 and 1277 cm^{-1} while in N-benzylamides [67] these modes are assigned between 1508 and 1513 cm^{-1}. In cocaine, these modes are predicted for the cationic species at 1528/1404 and for hydrochloride at 1490/1365 cm^{-1}. Here, both cationic and hydrochloride form of cocaine, as in species tropane, the N atom has sp^3 hybridization for which the normal internal coordinates corresponding to the N-H group is different from those species containing the N atom with sp^2 hybridization [66-70] because in this case the group N-H is planar. Hence, the in-plane deformation modes are not observed in the cationic and hydrochloride species.

CH modes. In the three cocaine species are expected the stretching, in-plane and out-of-plane deformation modes due to the C-H groups of the benzyl rings where the C atoms present sp^2 hybridization and, the stretching, out-of-plane deformation or rocking modes corresponding to the C atoms with sp^3

TABLE – 3 Observed and calculated wavenumbers (cm-1) and assignments for the free base, cationic and hydrochloride species of cocaine in gas phase.

Experimental							B3LYP/6-31G* Method[a]					
Hydrochloride				Free base			Free base		Cationic		Hydrochloride	
IR[c]	ATR[d]	FTIR[d]	Raman[e]	ATR[d]	FTIR[d]	Raman[e]	SQM[b]	Assignments	SQM[b]	Assignments	SQM[b]	Assignments
	3094vw			3093vw			3101	νC19-H40	3099	νC19-H40	3108	νC19-H40
							3092	νC18-H39	3097	νC18-H39	3091	νC18-H39
									3085	νC20-H41		
		3086w			3088w				3084	ν_aCH_3(C16)		
3076w							3075	νC21-H42	3077	νC21-H42	3077	νC21-H42
							3065	νC20-H41	3070	ν_aCH_3(C13)	3067	νC20-H41
3068sh									3067	νC22-H43		

									3056	ν_aCH$_3$(C13)	3058	ν_aCH$_3$(C13)
											3055	νC22-H43
											3055	ν_aCH$_3$(C16)
	3053vw						3053	νC22-H43	3052	ν_aCH$_3$(C16)	3051	ν_aCH$_3$(C13)
3043vw		3044sh			3047sh		3047	ν_aCH$_3$(C16)			3047	ν_aCH$_3$(C16)
				3034vw							3035	νC6-H23
3024vw	3023w	3020w					3018	ν_aCH$_3$(C16)	3022	ν_aCH$_2$(C9)		
		3009sh					3009	ν_aCH$_2$(C11)	3008	ν_aCH$_2$(C10)	3010	νC7-H24
									3006	νC8-H25	3006	ν_aCH$_2$(C9)
									3003	νC7-H24		
							2996	ν_aCH$_3$(C13)	2998	ν_aCH$_2$(C11)		
							2993	ν_aCH$_2$(C10)	2997	νC6-H23	2993	ν_aCH$_2$(C11)
	2982sh	2981sh			2985w		2988	νC6-H23	2989	νN5-H44	2991	ν_aCH$_2$(C10)
				2979w			2976	νC12-H32	2977	ν_sCH$_2$(C9)		
2969m				2973sh			2974	ν_aCH$_2$(C9)	2975	νC12-H32		
									2972	ν_sCH$_2$(C10)	2968	ν_sCH$_3$(C13)
							2965	νC7-H24	2970	ν_sCH$_3$(C13)	2963	ν_sCH$_2$(C10)
2958m	2959w	2959w			2955m		2954	ν_aCH$_3$(C13)	2969	ν_sCH$_3$(C16)	2958	ν_sCH$_2$(C9)
2956sh	2952sh						2951	ν_sCH$_2$(C9)	2950	ν_sCH$_2$(C11)	2957	νC12-H32
							2949	νC8-H25			2957	ν_sCH$_3$(C16)
	2943sh	2943sh		2945s			2946	ν_sCH$_3$(C16)			2943	ν_sCH$_2$(C11)
							2942	ν_sCH$_2$(C10)			2942	νC8-H25
				2933sh	2933sh		2938	ν_sCH$_2$(C11)				
2892w	2896w	2899w		2867w								
	2874w	2871w		2884w	2883w		2845	ν_sCH$_3$(C13)				
2856w				2852w	2850w							
2806w		2832sh		2806w	2798w							
	2542s	2539w									2089	νN5-H44
1766m	1727vs	1731vs		1733vs	1734vs	1744w	1760	νC14=O3	1733	νC15=O4	1763	νC14=O3
1737s	1710vs	1713vs	1717vs	1704vs	1707vs	1715vs	1719	νC15=O4	1692	νC14=O3	1719	νC15=O4
1603w	1597w	1598w	1598vs	1601w	1597w	1608vs	1608	νC18-C20	1605	νC18-C20	1608	νC18-C20
	1585w	1581w		1585w	1580w		1588	νC20-C22	1585	νC21-C22	1588	νC20-C22
	1541vw	1542vw			1522w				1528	ρN5-H44		
	1490sh	1489m	1489w	1493vw		1496sh	1495	βC20-H41	1494	βC20-H41	1495	βC20-H41
	1486m										1490	ρN5-H44
1477w	1477sh	1479sh		1478w			1478	δCH$_2$(C10)	1482	δCH$_2$(C9)	1483	δCH$_2$(C10)
		1466sh			1472w	1470sh	1474	δ_aCH$_3$(C13)	1468	δ_aCH$_3$(C13)	1466	δCH$_2$(C9)
	1458sh	1455s		1460sh			1461	δ_aCH$_3$(C16)			1463	δ_aCH$_3$(C16)
1452w	1450m		1459w	1450s	1447s		1455	δ_aCH$_3$(C13)	1454	δCH$_2$(C11)	1459	δCH$_2$(C11)
							1454	βC22-H43	1454	βC22-H43	1454	βC22-H43
	1444sh	1437sh		1445sh	1442sh		1454	δCH$_2$(C9)	1454	δ_aCH$_3$(C13)		
						1451s			1451	δCH$_2$(C11)	1451	δ_aCH$_3$(C13)
							1449	δCH$_2$(C11)	1449	δ_aCH$_3$(C16)	1443	δ_aCH$_3$(C16)
1440sh		1433s	1437sh				1447	δ_aCH$_3$(C16)	1448	δ_aCH$_3$(C16)	1442	δ_aCH$_3$(C13)
	1427m			1428sh	1432sh		1426	δ_sCH$_3$(C16)	1437	δ_sCH$_3$(C16)	1423	δ_sCH$_3$(C16)
		1423sh		1423sh	1416sh	1423m	1421	δ_sCH$_3$(C13)	1416	δ_sCH$_3$(C13)	1416	ρC12-H32
									1404	ρ'N5-H44	1409	δ_sCH$_3$(C13)

									3056	ν_aCH$_3$(C13)	3058	ν_aCH$_3$(C13)
											3055	νC22-H43
											3055	ν_aCH$_3$(C16)
	3053vw						3053	νC22-H43	3052	ν_aCH$_3$(C16)	3051	ν_aCH$_3$(C13)
3043vw		3044sh			3047sh		3047	ν_aCH$_3$(C16)			3047	ν_aCH$_3$(C16)
				3034vw							3035	νC6-H23
3024vw	3023w	3020w					3018	ν_aCH$_3$(C16)	3022	ν_aCH$_2$(C9)		
		3009sh					3009	ν_aCH$_2$(C11)	3008	ν_aCH$_2$(C10)	3010	νC7-H24
									3006	νC8-H25	3006	ν_aCH$_2$(C9)
									3003	νC7-H24		
							2996	ν_aCH$_3$(C13)	2998	ν_aCH$_2$(C11)		
							2993	ν_aCH$_2$(C10)	2997	νC6-H23	2993	ν_aCH$_2$(C11)
	2982sh	2981sh			2985w		2988	νC6-H23	2989	νN5-H44	2991	ν_aCH$_2$(C10)
				2979w			2976	νC12-H32	2977	ν_sCH$_2$(C9)		
2969m				2973sh			2974	ν_aCH$_2$(C9)	2975	νC12-H32		
									2972	ν_sCH$_2$(C10)	2968	ν_sCH$_3$(C13)
							2965	νC7-H24	2970	ν_sCH$_3$(C13)	2963	ν_sCH$_2$(C10)

2958m	2959w	2959w			2955m		2954	$\nu_aCH_3(C13)$	2969	$\nu_sCH_3(C16)$	2958	$\nu_sCH_2(C9)$
2956sh	2952sh						2951	$\nu_sCH_2(C9)$	2950	$\nu_sCH_2(C11)$	2957	νC12-H32
							2949	νC8-H25			2957	$\nu_sCH_3(C16)$
	2943sh	2943sh		2945s			2946	$\nu_sCH_3(C16)$			2943	$\nu_sCH_2(C11)$
							2942	$\nu_sCH_2(C10)$			2942	νC8-H25
				2933sh	2933sh		2938	$\nu_sCH_2(C11)$				
2892w	2896w	2899w		2867w								
	2874w	2871w		2884w	2883w		2845	$\nu_sCH_3(C13)$				
2856w				2852w	2850w							
2806w		2832sh		2806w	2798w							
	2542s	2539w									2089	νN5-H44
1766m	1727vs	1731vs		1733vs	1734vs	1744w	1760	νC14=O3	1733	νC15=O4	1763	νC14=O3
1737s	1710vs	1713vs	1717vs	1704vs	1707vs	1715vs	1719	νC15=O4	1692	νC14=O3	1719	νC15=O4
1603w	1597w	1598w	1598vs	1601w	1597w	1608vs	1608	νC18-C20	1605	νC18-C20	1608	νC18-C20
	1585w	1581w		1585w	1580w		1588	νC20-C22	1585	νC21-C22	1588	νC20-C22
	1541vw	1542vw			1522w				1528	ρN5-H44		
	1490sh	1489m	1489w	1493vw		1496sh	1495	βC20-H41	1494	βC20-H41	1495	βC20-H41
	1486m										1490	ρN5-H44
1477w	1477sh	1479sh		1478w			1478	$\delta CH_2(C10)$	1482	$\delta CH_2(C9)$	1483	$\delta CH_2(C10)$
		1466sh			1472w	1470sh	1474	$\delta_aCH_3(C13)$	1468	$\delta_aCH_3(C13)$	1466	$\delta CH_2(C9)$
	1458sh	1455s		1460sh			1461	$\delta_aCH_3(C16)$			1463	$\delta_aCH_3(C16)$
1452w	1450m		1459w	1450s	1447s		1455	$\delta_aCH_3(C13)$	1454	$\delta CH_2(C11)$	1459	$\delta CH_2(C11)$
							1454	βC22-H43	1454	βC22-H43	1454	βC22-H43
	1444sh	1437sh		1445sh	1442sh		1454	$\delta CH_2(C9)$	1454	$\delta_aCH_3(C13)$		
						1451s			1451	$\delta CH_2(C11)$	1451	$\delta_aCH_3(C13)$
							1449	$\delta CH_2(C11)$	1449	$\delta_aCH_3(C16)$	1443	$\delta_aCH_3(C16)$
1440sh		1433s	1437sh				1447	$\delta_aCH_3(C16)$	1448	$\delta_aCH_3(C16)$	1442	$\delta_aCH_3(C13)$
	1427m			1428sh	1432sh		1426	$\delta_sCH_3(C16)$	1437	$\delta_sCH_3(C16)$	1423	$\delta_sCH_3(C16)$
		1423sh		1423sh	1416sh	1423m	1421	$\delta_sCH_3(C13)$	1416	$\delta_sCH_3(C13)$	1416	ρC12-H32
									1404	ρ'N5-H44	1409	$\delta_sCH_3(C13)$
	756w	752m	754w	753w	766s		748	$\beta R_2(A3)$			747	νN5-C7
				743sh	742m		743	$\beta R_1(A3)$	742	$\beta R_2(A3)$	744	$\beta R_2(A3)$
	735sh	731vs	730w						738	νN5-C7		
	729s	718sh	722sh	717sh	723sh	728w	717	$\tau R_1(A2)$	718	γCOO(C15)	718	$\beta R_1(A3)$
710w		709sh		710s	711vs		713	γCOO(C15)	713	γCOO(C15)	715	γCOO(C15)
710w		709sh		710s	705vs				697	$\beta R_1(A3)$		
680sh	683w	680w		689w			682	$\beta R_3(A1)$	683	$\beta R_3(A1)$	685	$\beta R_3(A1)$
	676sh		680w	676w	679m	679w	677	$\tau R_1(A1)$	675	$\tau R_1(A1)$	676	$\tau R_1(A1)$
				651w	667m	651w	655	γCOO(C14)				
618w		632w	635w		640m		628	$\beta R_2(A1)$	627	$\beta R_2(A1)$	628	$\beta R_2(A1)$
		613w	613m		609m	617m	603	$\beta R_1(A3)$	609	$\tau R_2(A2)$	619	γN5-C13
		581w	583w		548m	559w	550	δO1C12C8			567	γCOO(C14)
		560w	565w								559	$\beta R_3(A2)$
		540w	545w		538sh				542	$\tau R_2(A2)$	542	δO1C12C8
		528sh			511m	517w	517	$\beta R_3(A2)$	511	δO1C12C8		
		486w	487w		498sh		497	$\beta R_2(A2)$	478	ρCOO(C15)	490	$\beta R_2(A2)$
		444vw			436vw		446	$\tau R_2(A1)$	439	$\tau R_2(A1)$	445	$\tau R_2(A1)$
		420w	420w		414sh	414w	415	$\beta R_3(A2)$	422	$\beta R_3(A2)$	415	$\tau R_2(A1)$
			390w		409w		406	δO1C12C11	400	$\tau R_3(A1)$	401	$\tau R_3(A1)$
			390w		396w		404	$\tau R_3(A1)$	390	$\tau R_1(A2)$	392	$\tau R_2(A2)$
							375	ρCOO(C14)	380	$\beta R_2(A2)$	382	ρCOO(C14)
			368w			364w	355	$\tau R_1(A2)$	361	$\tau R_1(A2)$	364	$\tau R_1(A2)$
			338w			332w	326	δC14O2C16	319	βN5-C13	334	δC14O2C16
			308vw			299w			309	$\beta R_2(A2)$	309	βN5-C13
						281w	288	$\tau R_2(A2)$			285	$\tau R_2(A2)$
			275w			281w	281	βC15-C17	274	$\tau R_2(A3)$	276	$\tau R_1(A2)$
			275w				265	γN5-C13	267	βC15-C17	264	βC15-C17
							254	$\tau R_1(A2)$				
			230w			237w			235	ρCOO(C14)		
									221	τO2-C14	221	$\tau R_1(A3)$
							208	$\tau R_1(A3)$			216	$\tau R_2(A3)$
			195sh			189sh	191	$\tau_wCH_3(C13)$	200	$\tau R_1(A3)$	199	$\tau R_2(A2)\tau R_2(A3)$
			183sh				181	$\tau R_1(A3)$	181	$\tau R_2(A2)$	178	τO2-C14
			179vw#			175s			168	$\tau_wCH_3(C13)$		

169w	162s#	161	$\tau R_2(A2)$			162	γC15-C17
154w#	159sh	158	τO2-C14	160	γC15-C17	159	$\tau R_2(A2)$
						149	$\tau_w CH_3(C13)$
139s		138	$\tau R_2(A2)$	134	$\tau R_2(A2)$		
127sh	126w#	122	$\tau_w CH_3(C16)$	124	$\tau_w CH_3(C16)$	128	$\tau R_2(A2)$
116w#				112	$\tau R_3(A2)$	117	$\tau_w CH_3(C16)$
99m#	108m	108	$\tau R_2(A2)$			99	$\tau R_1(A2)$
90m#	84m#	90	δC6C8C14	90	$\tau_w CH_3(C16)$	91	δCl45H44N5
71w#	75s#			76	τO1-C12	82	τN5-H44
71w#						65	τO1-C12
53w#	54m#	59	τ_wCOO(C15)	57	τ_wCOO(C14)		
	49sh#	48	$\tau R_2(A2)$				
43w3	49sh#	41	τ_wCOO(C14)	45	$\tau R_2(A2)$	42	τ_wCOO(C14)
33w#				30	τ_wCOO(C15)	34	$\tau R_2(A2)$
33w#	23vw#	24	$\tau R_1(A2)$	25	τC15-O1	24	τ_wCOO(C15)
	23vw#	21	τC15-O1			24	$\tau R_2(A2)$

Abbreviations: ν, stretching; β deformation in the plane; γ deformation out of plane; wag, wagging; τ, torsion; β_R, deformation ring τ_R, torsion ring; ρ, rocking; w, twisting; δ, deformation; a, antisymmetric; s, symmetric; (A_1), benzyl Ring1; (A_2), piperidine Ring2; (A_3), pyrrolidine Ring3. [a]This work, [b]From scaled quantum mechanics force field; [c]From Ref [62]; [d]From Ref [12,14,31]; [e]From Ref [63]. [#]From Ref [9], THz spectrum.

hyb

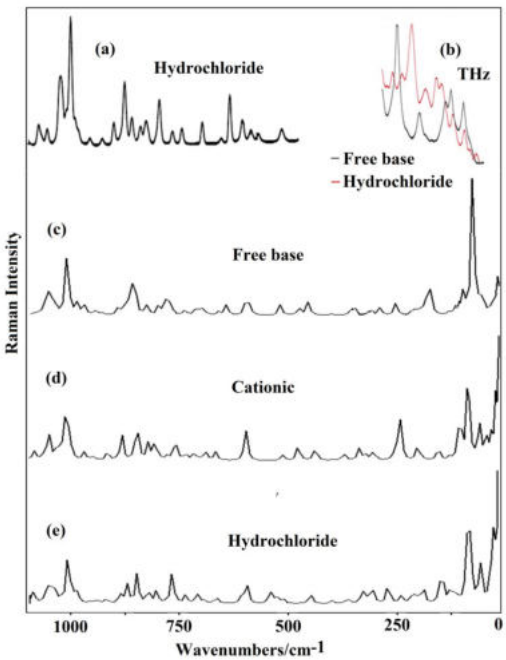

Figure 5. Comparisons between the experimental available Raman spectra of free base and hydrochloride species of cocaine in the solid states in the 1100-10 cm^{-1} [63] (a) and 400-24 cm^{-1} regions [9] with the corresponding predicted for the free base ©, cationic (d) and hydrochloride (e) species in the gas phase at B3LYP/6-31G** level of theory.

Obviously, the aromatic C-H stretching modes are assigned at higher wavenumbers than the corresponding aliphatic because they are predicted by SQM calculations between 3108 and 3053 cm^{-1} while the aliphatic C-H stretching modes are assigned between 3035 and 2942 cm^{-1} since they are predicted in these regions. The in-plane and out-of-plane deformation modes of C-H aliphatic for the three cocaine species are assigned as predicted by the calculations, this is between 1495/1161 and 1022/856 cm^{-1}, respectively. The aliphatic C-H rocking modes for the three species are assigned between 1398 and 1230 cm^{-1}, as can be seen in Table 3.

Ch$_3$ modes. In each cocaine species there are two CH_3 groups, hence, 18 vibration normal modes are expected. In the higher wavenumbers region the antisymmetric and symmetric modes were not identified, as was above explained, because the experimental available Raman spectrum only was reported from 2000 cm^{-1}. For all cocaine species, the antisymmetric and symmetric stretching modes are calculated as practically pure modes; hence, they were easily assigned to the bands observed between 3056 and 2845 cm^{-1}. In tropane, these modes are assigned between 3098 and 2966 cm^{-1}. Note that these modes in the cationic species are predicted at higher wavenumbers than the other ones, as was also observed in the same tropane species. The deformation modes in the tropane species are predicted between 1478 and 1400 cm^{-1}, in cocaine species between 1474 and 1409 cm^{-1}, for this reason, they were assigned in these regions, as detailed in Table 3. On the other hand, the rocking modes are predicted between 1194 and 1134 cm^{-1} while in the tropane species between 1183 and 1128 cm^{-1}. For the cocaine species, the twisting modes are predicted between 191 and 117 cm^{-1} while in the tropane species are assigned between 205 and 151 cm^{-1}. Hence, these modes for each species were assigned as predicted the SQM calculations. In species containing these CH_3 groups those modes were assigned in the same regions [39,67].

Ch$_2$ modes. In each cocaine species there are three CH_2 groups, hence, twelve vibration normal modes related to these groups are expected for each species. Here, the symmetries of the stretching modes were not determined because the experimental available Raman spectrum only was reported from 2000 cm^{-1}. In the cocaine species, the two stretching modes are predicted between 3009 and 2938 while in tropane species these modes are predicted between 3024 and 2911 cm^{-1}. From the same way, in cocaine species the deformation, wagging, rocking and twisting modes are predicted, in some cases mixed with other modes, in the 1483/1449, 1382/1242, 1230/1167 and 933/744 cm^{-1} regions, respectively while, in the tropane species, these modes were assigned respectively to the set of bands between 1485/1442, 1385/1274, 1274/1142 and 967/639 cm^{-1}. In compounds containing this group those modes were assigned in the same regions [39-41,59,67,69-71]. Thus, for the three cocaine species those modes were clearly assigned in the regions predicted by SQM calculations, as indicated in Table 3.

Skeletal modes. In the cocaine species, the N5-CH_3 stretching modes are predicted at 1113, 1058 and 1052 cm^{-1} while in the tropane species these modes were assigned to the IR bands at 1128, 1086 and 1031 cm^{-1}. Hence, the very strong IR band observed at 1111 cm^{-1} in the spectrum of hydrochloride and the ATR band with medium intensity at 1053 cm^{-1} for the same species are clearly assigned to these stretching modes, as detailed in Table 3. The N5-C6 and N5-C7 stretching modes corresponding to the bicyclic rings are predicted in different regions, as was also observed in tropane species. Hence, in the hydrochloride species those modes are predicted at 929 and 772 while in the species corresponding to tropane at 761 and 710 cm^{-1}, in the cationic cocaine species at 782 and 697 cm^{-1} while in tropane at 733 and 673 cm^{-1} and, in the free base at 955 and 772 cm^{-1} while in tropane species at 998 and 750 cm^{-1}. hence, Then, in the three tropane species the IR bands at 981, 776, 729, 706 and 680 cm^{-1} are easily assigned to those stretching modes while, for cocaine, the pairs of IR bands at 951/777, 922/747, 786/731 cm^{-1} are associated with the N5-C6 and N5-C7 stretching modes, as shown in Table 3. For the benzyl rings are expected three deformations (β_{R1}(A1), β_{R2}(A1) and β_{R3}(A1)) and three torsions (τ_{R1}(A1), τ_{R2}(A1) and τ_{R3}(A1)) rings, for the piperidine three deformations (τ_{R1}(A2), τ_{R2}(A2) and τ_{R3}(A2)) and three torsions (β_{R1}(A2), β_{R2}(A2) and β_{R3}(A2)) rings while for the pyrrolidine rings only two deformations (τ_{R1}(A3), τ_{R2}(A3)) and two torsions (τ_{R1}(A3) and τ_{R2}(A3)) rings are expected. In this case, the redundant internal coordinates was identified as β_{R1}(A2) and, for this reason, it was removed. Table 3 shows that these vibration modes are all predicted in some case mixed among them and between 1065 and 24 cm^{-1}. The SQM calculations and the assignments reported for species containing rings [32,47-51] were employed to assign those vibration modes. For the three cocaine species, practically all vibration modes observed in the lower wavenumbers 400-24 cm^{-1} region were assigned, as observed in Table 3; because the bands observed in the experimental available Raman spectrum [63] and in the terahertz spectrum recorded for hydrochloride cocaine by Davies et al [9] were also considered.

FORCE CONSTANTS

For the free base, cationic and hydrochloride species of cocaine were calculated the force constants by using their corresponding force fields calculated at the B3LYP/6-31G* level of theory with the SQMFF procedure [52] and the Molvib program [53]. The scaled internal force constants can be seen in **Table 4** together with those reported for the three species of tropane alkaloid in both media and at the same level of theory. First, we analyzed the force constants values for the three cocaine species. Here, the f(N-H) constant for the cationic species in both media are higher than the corresponding to the hydrochloride species, as observed in the two tropane species. In the cationic cocaine species in gas phase, the N-H distance is 1.044 Å higher than the corresponding to the tropane species in the same medium (1.025 Å) while for the hydrochloride cocaine species is 1.110 Å lower than the corresponding to the tropane species (1.135 Å). Hence, the calculated bond lengths justify those values. Here, a result very interesting is observed in the f(νN-CH_3) constants for the free base because their values in both media are the same than the corresponding to the tropane species [32] while the lower values are observed for the cationic species in both media. In general, we observed the same behaviours of the f(νC-H), f(νC-C), and force constants for the three species of cocaine and tropane in both media, as can be seen in **Figure S10**. In particular, we observed for the cocaine and tropane species slightly increase in the f(νCH_2), f(νCH_3), f(νC-H) and f(νC-C) force constants values in aqueous solution, as also was observed for the tropane species (Table 4). Probably, these variations are related to the MK charges that experiment the C atoms belong to those groups because a decreasing in their values is observed in solution. Here, it is necessary to clarify that the C atoms involved in the force constants presented in Table 4 correspond to the piperideine and pyrrolidine rings, with exception of the C atoms belong to the CH_3 groups.

CONCLUSIONS

In this work, the structural, electronic, topological and vibrational properties of the free base, cationic and hydrochloride species of cocaine were studied in gas and aqueous solution phases by using the hybrid B3LYP/6-31G* calculations. In solution, the SCRF and PCM methods were employed together with the SMD model in order to obtain the solvation energies for the three species and where the higher values were predicted for the cationic species. The calculations in both media do not evidence the fast N-methyl inversion for none of the cocaine species, contrary to the observed for the cationic and hydrochloride species of tropane.

The NBO and AIM calculations support the high stabilities observed for the cationic species in both media while their higher gap energy could justify their low reactivities. The AIM analysis predicted O--O interactions for the hydrochloride species in both media that probably explain the high reactivities of this species in both media, as suggested by their gap energy values.

The SQMFF methodology, the normal internal coordinates and the experimental available ATR, FTIR, FTRaman and Terahertz spectra for the free base and the hydrochloride species were used to compute the force fields and to perform the complete vibrational assignments of those three species of cocaine. The force constants and the complete assignments of the 123, 126 and 129 vibration normal modes expected for the free base, cationic and hydrochloride species respectively are reported here for first time. The predicted IR spectrum for cocaine hydrochloride reveals that in the solid state this species is in their cationic form, as evidenced by their experimental IR spectrum.

TABLE – 4

Comparison of main scaled internal force constants for the free base, cationic and hydrochloride cocaine species in gas and aqueous solution phases compared with those calculated for the tropane species.

B3LYP/6-31G*						
Cocaine[a]						
Force constant	Free base		Cationic		Hydrochloride	
	Gas	PCM	Gas	PCM	Gas	PCM
f(ν N-H)			4.91	5.55	3.23	4.79
f(ν N-CH₃)	4.69	4.52	4.17	4.23	4.31	4.17
f(ν C-N)	4.20	4.01	3.41	3.51	3.71	3.54
f(ν CH₂)	4.85	4.87	4.91	4.93	4.88	4.93
f(ν CH₃)	4.86	4.92	5.07	5.09	5.04	5.08
f(ν C-H)	4.86	4.91	4.93	5.02	4.91	4.98
f(ν C-C)	3.94	3.98	4.06	4.09	4.08	4.11
f(δ CH₂)	0.74	0.72	0.75	0.73	0.75	0.73
f(δ CH₃)	0.58	0.56	0.57	0.56	0.57	0.56
Tropane[a]						
Force constant	Free base		Cationic		Hydrochloride	
	Gas	PCM	Gas	PCM	Gas	PCM
f(ν N-H)			5.97	5.98	2.70	4.69
f(ν N-CH₃)	4.69	4.52	4.09	4.21	4.42	4.26
f(ν C-N)	4.16	3.97	3.11	3.35	3.73	3.48
f(ν CH₂)	4.78	4.78	4.88	4.88	4.85	4.87
f(ν CH₃)	4.72	4.79	5.10	5.13	5.03	5.11
f(ν C-H)	4.78	4.82	4.92	4.99	4.90	4.96
f(ν C-C)	4.05	4.06	4.17	4.21	4.16	4.20
f(δ CH₂)	0.74	0.72	0.75	0.72	0.74	0.73
f(δ CH₃)	0.58	0.57	0.56	0.56	0.56	0.56

Units are mdyn $Å^{-1}$ for stretching and mdyn Å rad^{-2} for angle deformations, [a]This work

The analyses of the descriptors suggest that the cation cocaine in both media is most electrophilic and reactive than the cation tropane increasing notably their reactivity. However, the nucheophilicity indexes for the tropane alkaloid in both media are comparable to those observed for toxics substances as saxitoxin and cation pyridonium. Probably these results for tropane, different from the observed for cocaine species, suggest that the modifications in the stereochemistry of tropane generate a loss in their potency, as was reported in the literature.

ACKNOWLEDGEMENTS

This work was supported with grants from CIUNT Project Nş 26/D207 (Consejo de Investigaciones, Universidad Nacional de Tucumán). The authors would like to thank Prof. Tom Sundius for his permission to use MOLVIB.

Supporting Material

Table S1. Atomic MK charges and molecular electrostatic potentials for the most stable free base, cationic and hydrochloride structures of cocaine by using the hybrid B3LYP/6-31G* level of theory.

Atoms	MK charges						MEP					
	Free base		Cationic		Hydrochloride		Free base		Cationic		Hydrochloride	
	Gas	PCM	Gas	PCM	Gas	PCM	Gas	PCM	Gas	PCM	Gas	PCM
1 O	-0.507	-0.492	-0.473	-0.455	-0.534	-0.535	-22.280	-22.281	-22.157	-22.154	-22.269	-22.263
2 O	-0.364	-0.366	-0.294	-0.298	-0.280	-0.324	-22.277	-22.275	-22.131	-22.136	-22.269	-22.267
3 O	-0.534	-0.549	-0.555	-0.543	-0.460	-0.468	-22.339	-22.342	-22.181	-22.184	-22.333	-22.333
4 O	-0.508	-0.520	-0.470	-0.476	-0.502	-0.510	-22.338	-22.341	-22.225	-22.231	-22.329	-22.327
5 N	-0.273	-0.290	-0.159	-0.107	0.177	0.343	-18.362	-18.361	-18.095	-18.085	-18.248	-18.229
6 C	0.204	0.185	0.191	0.183	0.095	0.078	-14.705	-14.704	-14.525	-14.521	-14.657	-14.646
7 C	0.150	0.180	0.097	0.117	-0.008	-0.030	-14.710	-14.711	-14.531	-14.526	-14.662	-14.650
8 C	-0.666	-0.701	-0.695	-0.703	-0.403	-0.419	-14.726	-14.724	-14.573	-14.569	-14.696	-14.687
9 C	-0.150	-0.131	-0.140	-0.110	-0.111	-0.137	-14.739	-14.738	-14.582	-14.578	-14.697	-14.688
10 C	-0.181	-0.235	-0.133	-0.169	-0.150	-0.148	-14.740	-14.740	-14.583	-14.579	-14.698	-14.689
11 C	-0.452	-0.460	-0.380	-0.378	-0.257	-0.239	-14.747	-14.746	-14.588	-14.584	-14.719	-14.709
12 C	0.684	0.651	0.578	0.555	0.657	0.627	-14.680	-14.678	-14.533	-14.528	-14.652	-14.645
13 C	-0.439	-0.410	-0.449	-0.451	-0.389	-0.451	-14.718	-14.719	-14.539	-14.534	-14.674	-14.665
14 C	0.882	0.911	0.853	0.850	0.667	0.741	-14.620	-14.620	-14.466	-14.468	-14.607	-14.605
15 C	0.599	0.627	0.546	0.536	0.580	0.606	-14.616	-14.617	-14.505	-14.507	-14.608	-14.604
16 C	-0.069	-0.081	-0.171	-0.155	-0.164	-0.129	-14.686	-14.684	-14.569	-14.572	-14.698	-14.691
17 C	0.007	-0.026	0.015	0.038	0.039	0.000	-14.729	-14.728	-14.631	-14.634	-14.726	-14.722
18 C	-0.130	-0.130	-0.123	-0.136	-0.141	-0.133	-14.736	-14.736	-14.644	-14.648	-14.733	-14.730
19 C	-0.130	-0.129	-0.126	-0.135	-0.127	-0.104	-14.736	-14.736	-14.639	-14.642	-14.734	-14.731
20 C	-0.109	-0.106	-0.105	-0.101	-0.103	-0.105	-14.735	-14.736	-14.649	-14.652	-14.734	-14.731
21 C	-0.115	-0.112	-0.120	-0.119	-0.121	-0.135	-14.736	-14.736	-14.647	-14.650	-14.735	-14.733
22 C	-0.109	-0.106	-0.078	-0.085	-0.101	-0.088	-14.732	-14.732	-14.644	-14.647	-14.730	-14.727
23 H	0.067	0.077	0.098	0.098	0.047	0.060	-1.118	-1.117	-0.942	-0.937	-1.074	-1.063
24 H	0.090	0.088	0.113	0.106	0.111	0.115	-1.121	-1.121	-0.947	-0.942	-1.077	-1.066
25 H	0.169	0.178	0.221	0.220	0.141	0.131	-1.110	-1.109	-0.963	-0.960	-1.079	-1.071
26 H	0.068	0.066	0.086	0.078	0.057	0.062	-1.124	-1.123	-0.972	-0.968	-1.085	-1.076
27 H	0.070	0.073	0.110	0.106	0.067	0.084	-1.122	-1.121	-0.969	-0.964	-1.082	-1.073
28 H	0.062	0.079	0.094	0.105	0.075	0.080	-1.123	-1.122	-0.970	-0.965	-1.083	-1.074
29 H	0.073	0.085	0.090	0.094	0.068	0.067	-1.126	-1.125	-0.973	-0.969	-1.086	-1.077
30 H	0.105	0.109	0.142	0.146	0.087	0.089	-1.126	-1.125	-0.970	-0.966	-1.096	-1.087
31 H	0.149	0.155	0.136	0.134	0.106	0.113	-1.134	-1.133	-0.972	-0.968	-1.106	-1.097
32 H	0.024	0.036	0.053	0.060	-0.023	-0.014	-1.119	-1.118	-0.977	-0.973	-1.097	-1.089
33 H	0.138	0.132	0.209	0.210	0.146	0.159	-1.125	-1.124	-0.938	-0.932	-1.068	-1.060
34 H	0.156	0.150	0.201	0.200	0.159	0.177	-1.119	-1.119	-0.939	-0.933	-1.076	-1.067
35 H	0.162	0.157	0.195	0.194	0.164	0.184	-1.119	-1.119	-0.939	-0.933	-1.072	-1.065
36 H	0.101	0.105	0.157	0.151	0.114	0.110	-1.105	-1.103	-0.991	-0.994	-1.113	-1.109
37 H	0.078	0.085	0.127	0.120	0.135	0.128	-1.110	-1.107	-0.990	-0.993	-1.124	-1.118
38 H	0.077	0.083	0.128	0.120	0.101	0.092	-1.110	-1.107	-0.990	-0.994	-1.117	-1.112
39 H	0.123	0.128	0.136	0.140	0.123	0.123	-1.110	-1.110	-1.020	-1.024	-1.107	-1.104
40 H	0.150	0.153	0.129	0.126	0.154	0.150	-1.111	-1.111	-1.012	-1.015	-1.111	-1.108
41 H	0.117	0.117	0.135	0.134	0.115	0.115	-1.106	-1.107	-1.024	-1.026	-1.105	-1.102
42 H	0.116	0.116	0.133	0.132	0.122	0.126	-1.107	-1.107	-1.021	-1.023	-1.107	-1.105
43 H	0.119	0.117	0.132	0.133	0.118	0.115	-1.104	-1.104	-1.021	-1.024	-1.103	-1.101
44 H			0.368	0.337	0.119	0.010			-0.833	-0.827	-0.986	-0.979
45 Cl					-0.670	-0.718					-64.514	-64.535

Table S2. NPA charges and Wiberg indexes for the most stable free base, cationic and hydrochloride structures of cocaine by using the hybrid B3LYP/6-31G* level of theory.

Atoms	NPA charges						Wiberg indexes					
	Free base		Cationic		Hydrochloride		Free base		Cationic		Hydrochloride	
	Gas	PCM	Gas	PCM	Gas	PCM	Gas	PCM	Gas	PCM	Gas	PCM
1 O	-0.544	-0.543	-0.569	-0.563	-0.538	-0.534	2.159	2.162	2.109	2.122	2.157	2.164
2 O	-0.556	-0.553	-0.502	-0.509	-0.559	-0.559	2.134	2.141	2.224	2.213	2.145	2.142
3 O	-0.595	-0.600	-0.644	-0.637	-0.582	-0.564	2.040	2.028	2.011	2.010	2.053	2.063
4 O	-0.613	-0.617	-0.595	-0.601	-0.618	-0.621	2.015	2.007	2.040	2.028	2.011	2.004
5 N	-0.524	-0.519	-0.483	-0.475	-0.503	-0.490	3.091	3.085	3.418	3.431	3.359	3.388
6 C	-0.058	-0.059	-0.048	-0.047	-0.056	-0.051	3.914	3.916	3.856	3.854	3.870	3.864
7 C	-0.066	-0.068	-0.054	-0.053	-0.054	-0.052	3.917	3.918	3.852	3.849	3.867	3.863

8 C	-0.378	-0.377	-0.396	-0.395	-0.392	-0.390	3.943	3.944	3.922	3.923	3.935	3.935
9 C	-0.490	-0.491	-0.492	-0.491	-0.486	-0.489	3.892	3.891	3.866	3.865	3.881	3.878
10 C	-0.491	-0.492	-0.493	-0.493	-0.490	-0.491	3.895	3.894	3.870	3.869	3.884	3.881
11 C	-0.482	-0.482	-0.504	-0.505	-0.504	-0.504	3.890	3.890	3.874	3.873	3.867	3.867
12 C	0.084	0.085	0.088	0.087	0.089	0.086	3.837	3.835	3.846	3.843	3.851	3.851
13 C	-0.470	-0.473	-0.477	-0.476	-0.475	-0.473	3.815	3.816	3.725	3.722	3.745	3.737
14 C	0.848	0.845	0.854	0.847	0.838	0.826	3.826	3.827	3.822	3.829	3.837	3.845
15 C	0.819	0.817	0.821	0.820	0.830	0.822	3.833	3.834	3.824	3.825	3.826	3.829
16 C	-0.323	-0.322	-0.328	-0.328	-0.325	-0.326	3.723	3.720	3.677	3.680	3.690	3.693
17 C	-0.167	-0.167	-0.188	-0.184	-0.168	-0.172	3.998	3.998	3.993	3.995	3.998	3.998
18 C	-0.186	-0.185	-0.173	-0.175	-0.185	-0.184	3.936	3.937	3.932	3.932	3.937	3.937
19 C	-0.191	-0.191	-0.191	-0.196	-0.181	-0.183	3.932	3.932	3.939	3.941	3.931	3.930
20 C	-0.239	-0.239	-0.230	-0.230	-0.240	-0.240	3.947	3.947	3.941	3.942	3.947	3.947
21 C	-0.238	-0.238	-0.233	-0.234	-0.236	-0.236	3.947	3.947	3.943	3.944	3.946	3.946
22 C	-0.214	-0.213	-0.192	-0.195	-0.210	-0.209	3.948	3.948	3.940	3.940	3.947	3.947
23 H	0.262	0.260	0.282	0.283	0.283	0.287	0.934	0.935	0.922	0.922	0.922	0.920
24 H	0.251	0.251	0.281	0.281	0.278	0.279	0.939	0.939	0.923	0.923	0.925	0.924
25 H	0.283	0.282	0.318	0.316	0.304	0.302	0.923	0.923	0.902	0.903	0.910	0.912
26 H	0.245	0.245	0.269	0.269	0.253	0.255	0.942	0.941	0.929	0.929	0.937	0.936
27 H	0.245	0.246	0.278	0.279	0.261	0.265	0.941	0.941	0.924	0.923	0.933	0.931
28 H	0.241	0.241	0.274	0.276	0.258	0.260	0.944	0.943	0.926	0.925	0.935	0.934
29 H	0.242	0.242	0.267	0.267	0.251	0.254	0.943	0.943	0.930	0.930	0.938	0.937
30 H	0.242	0.242	0.284	0.285	0.261	0.263	0.944	0.943	0.921	0.920	0.934	0.932
31 H	0.269	0.270	0.268	0.269	0.293	0.296	0.931	0.930	0.931	0.930	0.918	0.916
32 H	0.249	0.251	0.262	0.265	0.241	0.245	0.942	0.941	0.935	0.934	0.946	0.944
33 H	0.191	0.192	0.252	0.254	0.226	0.226	0.968	0.967	0.937	0.937	0.950	0.950
34 H	0.230	0.231	0.264	0.264	0.271	0.272	0.948	0.948	0.931	0.931	0.929	0.929
35 H	0.230	0.230	0.264	0.265	0.255	0.263	0.949	0.949	0.931	0.931	0.936	0.933
36 H	0.221	0.221	0.245	0.245	0.217	0.218	0.952	0.952	0.940	0.941	0.954	0.953
37 H	0.219	0.220	0.232	0.230	0.252	0.251	0.955	0.954	0.948	0.949	0.939	0.940
38 H	0.219	0.221	0.233	0.232	0.218	0.218	0.955	0.954	0.948	0.948	0.955	0.955
39 H	0.256	0.256	0.262	0.262	0.254	0.255	0.937	0.937	0.933	0.933	0.938	0.937
40 H	0.263	0.263	0.249	0.247	0.263	0.266	0.933	0.933	0.940	0.941	0.932	0.931
41 H	0.239	0.239	0.253	0.252	0.240	0.240	0.944	0.944	0.937	0.938	0.944	0.944
42 H	0.240	0.240	0.250	0.248	0.242	0.243	0.944	0.944	0.939	0.940	0.943	0.942
43 H	0.238	0.237	0.251	0.251	0.239	0.239	0.945	0.945	0.938	0.938	0.944	0.944
44 H			0.493	0.491	0.436	0.465			0.762	0.764	0.820	0.796
45 Cl					-0.751	-0.828					0.455	0.322

Table S3. Main donor-acceptor energy interactions (in kJ/mol) for the free base, cationic and hydrochloride structures of cocaine by using the hybrid B3LYP/6-31G* level of theory.

Delocalization	Free base		Cationic		Hydrochloride	
	Gas	PCM	Gas	PCM	Gas	PCM
*σN5-C6→ LP*H44*					44.81	54.30
*σN5-C7→ LP*H44*					58.94	60.99
*σN5-C13→ LP*H44*					63.54	69.26
$\Delta ET_{\sigma\to LP*}$					**167.29**	**184.55**
*π (2)C17-C19→π*O4-C15*	95.55	96.56	110.94	107.51	99.23	102.74
*π (2)C17-C19→π*C18-C20*	87.61	87.32	82.56	82.60	88.45	88.16
*π (2)C17-C19→π*C21-C22*	77.46	77.58	71.27	71.81	76.33	75.45
π (2)C18-C20→π C17-C19*	78.79	78.29	80.51	81.01	77.75	77.08
*π (2)C18-C20→π*C21-C22*	90.20	90.16	89.79	89.66	89.70	89.54
π (2) C21-C22→π C17-C19*	92.88	93.30	101.53	100.19	94.26	95.51
*π (2) C21-C22→π*C18-C20*	76.12	75.95	73.23	73.86	76.20	76.03
$\Delta ET_{\pi\to\pi*}$	**598.62**	**599.16**	**609.82**	**606.64**	**601.92**	**604.51**
*π*O4-C15→π* C17-C19*	385.94	384.27	279.22	260.08	304.01	287.33
π C17-C19→π*C18-C20*			890.55	890.88		
$\Delta ET_{\pi*\to\pi*}$	**385.94**	**384.27**	**1169.77**	**1150.96**	**304.01**	**287.33**
*LP(2)O1 → σ*O4-C15*	205.36	210.13	165.15	183.13	194.29	36.41
*LP(2)O2 → σ*O3-C14*	200.97	209.04	264.05	250.09	200.47	206.49
*LP(2)O3 → σ*O2-C14*	145.34	137.69	118.59	124.77	140.78	136.39
*LP(2)O3 → σ*N5-C14*			75.16	42.85		
*LP(2)O3 → σ*C8-C14*	81.64	78.63	56.85	64.54	88.57	89.12
*LP(2)O4 → σ*O1-C15*	137.02	132.13	152.49	141.49	139.03	134.60
*LP(2)O4 → σ*C15-C17*	75.24	73.28	70.73	70.68	73.53	72.19
$\Delta ET_{LP\to\sigma*}$	**845.57**	**840.89**	**903.01**	**877.55**	**836.67**	**675.20**

*LP(1)N5 → LP*H44*					1323.30	1540.71
*LP(4)Cl45 → LP*H44*					494.24	244.49
$\Delta ET_{LP\rightarrow LP*}$					**1817.54**	**1785.20**
ΔE_{Total}	**1830.13**	**1824.32**	**2682.60**	**2635.15**	**3727.43**	**3536.79**

Table S4. Analysis of the topological properties for the free base, cationic and hydrochloride structures of cocaine by using the hybrid B3LYP/6-31G* level of theory.

Free base/Gas							
Parameter (a.u.)	**O3---H31**	RCPN	RCP1	RCP2	RCP3		
$\rho(r_c)$	0.0082	0.0080	0.0202	0.0194	0.0393		
$\nabla^2\rho(r_c)$	0.0316	0.0348	0.1617	0.1252	0.2660		
λ_1	-0.0069	-0.0052	-0.0152	-0.0131	-0.0399		
λ_2	-0.0036	0.0043	0.0878	0.0595	0.1489		
λ_3	0.0422	0.0356	0.0892	0.0787	0.1569		
$\lvert\lambda_1\rvert/\lambda_3$	0.1635	0.1461	0.1704	0.1665	0.2543		
Distance (Ĺ)	2.627						
Free base/PCM							
Parameter (a.u.)	**O3---H31**	RCPN	RCP1	RCP2	RCP3		
$\rho(r_c)$	0.0074	0.0074	0.0201	0.0193	0.0395		
$\nabla^2\rho(r_c)$	0.0294	0.0307	0.1612	0.1236	0.2654		
λ_1	-0.0059	-0.0053	-0.0152	-0.0133	-0.0402		
λ_2	-0.0014	0.0016	0.0873	0.0587	0.1469		
λ_3	0.0367	0.0343	0.0890	0.0782	0.1586		
$\lvert\lambda_1\rvert/\lambda_3$	0.1608	0.1545	0.1708	0.1701	0.2535		
Distance (Ĺ)	2.690						
Cation/Gas							
Parameter (a.u.)	**O3---H44**	RCPN	RCP1	RCP2	RCP3		
$\rho(r_c)$	0.0419	0.0165	0.0201	0.0188	0.0374		
$\nabla^2\rho(r_c)$	0.1304	0.0989	0.1614	0.1164	0.2535		
λ_1	-0.0645	-0.0123	-0.0152	-0.0127	-0.0372		
λ_2	-0.0631	0.0479	0.0877	0.0551	0.1442		
λ_3	0.2580	0.0632	0.0889	0.0741	0.1465		
$\lvert\lambda_1\rvert/\lambda_3$	0.2500	0.1946	0.1710	0.1714	0.2539		
Distance (Ĺ)	1.778						
Cation/PCM							
Parameter (a.u.)	**O3---H44**	RCPN1	**C19---H38**	RCPN1	RCP1	RCP2	RCP3
$\rho(r_c)$	0.0298	0.0145	0.0005	0.0005	0.0201	0.0188	0.0377
$\nabla^2\rho(r_c)$	0.0894	0.0827	0.0021	0.0025	0.1612	0.1174	0.2563
λ_1	-0.0402	-0.0104	-0.0002	-0.0001	-0.0152	-0.0128	-0.0378
λ_2	-0.0388	0.0378	-0.0001	0.0002	0.0872	0.0559	0.1455
λ_3	0.1685	0.0553	0.0024	0.0024	0.0891	0.0743	0.1485
$\lvert\lambda_1\rvert/\lambda_3$	0.2386	0.1881	0.0833	0.0417	0.1706	0.1723	0.2545
Distance (Ĺ)	1.942		4.038				

Table S5. Analysis of the topological properties for the free base, cationic and hydrochloride structures of cocaine by using the hybrid B3LYP/6-31G* level of theory.

Hydrochloride/GAS											
Parameter (a.u.)	**O3---O1**	RCPN1	**Cl45---H31**	RCPN2	**Cl45---H37**	RCPN3	**Cl45---H44**	RCPN4	RCP1	RCP2	RCP3
$\rho(r_c)$	0.0143	0.0126	0.0105	0.0092	0.0083	0.0061	0.0603	0.0092	0.0202	0.0189	0.0381
$\nabla^2\rho(r_c)$	0.0501	0.0629	0.0341	0.0376	0.0276	0.0253	0.0984	0.0376	0.1617	0.1186	0.2580
λ_1	-0.0124	-0.0100	-0.0086	-0.0068	-0.0067	-0.0039	-0.0906	-0.0068	-0.0152	-0.0127	-0.0377
λ_2	-0.0109	0.0172	-0.0064	0.0080	-0.0062	0.0058	-0.0900	0.0080	0.0879	0.0553	0.1459
λ_3	0.0734	0.0557	0.0492	0.0363	0.0405	0.0234	0.2789	0.0363	0.0891	0.0759	0.1498
$\lvert\lambda_1\rvert/\lambda_3$	0.1689	0.1795	0.1748	0.1873	0.1654	0.1667	0.3248	0.1873	0.1706	0.1673	0.2517
Distance (Ĺ)	2.750		2.744		2.838		1.843				
Hydrochloride/PCM											
Parameter (a.u.)	**O3---O1**	RCPN1	**Cl45---H31**	RCPN2	**Cl45---H37**	RCPN3	**Cl45---H44**	RCPN4	RCP1	RCP2	RCP3
$\rho(r_c)$	0.0141	0.0126			0.0034	0.0027	0.0369	0.0027	0.0201	0.0188	0.0380
$\nabla^2\rho(r_c)$	0.0487	0.0616			0.0100	0.0107	0.0728	0.0107	0.1612	0.1176	0.2578
λ_1	-0.0126	-0.0095			-0.0023	-0.0006	-0.0453	-0.0006	-0.0152	-0.0128	0.0375
λ_2	-0.0105	0.0164			-0.0021	0.0026	-0.0451	0.0026	0.0873	0.0545	0.1450
λ_3	0.0718	0.0548			0.0144	0.0087	0.1632	0.0087	0.0889	0.0758	0.1502
$\lvert\lambda_1\rvert/\lambda_3$	0.1755	0.1734			0.1597	0.0690	0.2776	0.0690	0.1710	0.1689	-0.2497
Distance (Ĺ)	2.755		3.153		3.309		2.088				

Table S6. Calculated HOMO and LUMO orbitals. energy band gap. chemical potential (μ). electronegativity (χ). global hardness (η). global softness (*S*). global electrophilicity index (ω) and global nucleophilicity index ( ) for the free base, cationic and hydrochloride structures of cocaine by using the hybrid B3LYP/6-31G* level of theory.

Cocaine[a]						
Frontier orbitals	Free base		Cationic		Hydrochloride	
	Gas	PCM	Gas	PCM	Gas	PCM
HOMO	-5.9267	-6.0125	-9.3162	-9.2302	-1.1856	-4.9833
LUMO	-1.0687	-1.0638	-3.8694	-3.7642	-0.0562	-1.3020
GAP	-4.858	-4.9487	-5.4468	-5.4660	-1.1294	-3.6813
Descriptors (eV)						
	-2.4290	-2.4744	-2.7234	-2.7330	-0.5647	-1.8407
	-3.4977	-3.5382	-6.5928	-6.4972	-0.6209	-3.1427
	2.4290	2.4744	2.7234	2.7330	0.5647	1.8407
S	0.2058	0.2021	0.1836	0.1829	0.8854	0.2716
	2.5183	2.5297	7.9799	7.7229	0.3413	2.6828
	-8.4959	-8.7546	-17.9548	-17.7568	-0.3506	-5.7845
Tropane alkaloid[a]						
Frontier orbitals (eV)	Free base		Cationic		Hydrochloride	
	Gas	PCM	Gas	PCM	Gas	PCM
HOMO	-5.4945	-5.6725	-12.9365	-12.9433	-5.5910	-4.9043
LUMO	2.0561	1.9886	-3.3770	-3.4183	1.2336	1.0076
GAP	-7.5506	-7.6611	-9.5595	-9.5250	-6.8246	-5.9119
Descriptors (eV)						
	-3.7753	-3.8306	-4.7798	-4.7625	-3.4123	-2.9560
	-1.7192	-1.8420	-8.1567	-8.1808	-2.1787	-1.9483
	3.7753	3.8306	4.7798	4.7625	3.4123	2.9560
S	0.1324	0.1305	0.1046	0.1050	0.1465	0.1691
	0.3914	0.4429	6.9598	7.0263	0.6955	0.6421
	-6.4905	-7.0557	-38.9872	-38.9613	-7.4343	-5.7592
Other species with different biological activities						
Frontier orbitals	thione[b]	thiol[b]	Cidofovir[c]	brincidofovir[c]	STX	Piridonium
HOMO	-6.4443	-6.8847	-5.9366	-5.5435	-13.656	-13.0216
LUMO	-2.7918	-2.6194	-0.6401	-1.772	-7.1273	-7.0153
GAP	-3.6525	-4.2653	-5.2965	-3.7715	-6.5287	-6.0063
Descriptors (eV)						
	-1.8263	-2.1327	-2.6483	-1.8858	-3.2644	-3.0032
	-4.6180	-4.7521	-3.2884	-3.6578	-10.3917	-10.0185
	1.8263	2.1327	2.6483	1.8858	3.2644	3.0032
S	0.2738	0.2345	0.1888	0.2651	0.1532	0.1665
	5.8388	5.2943	2.0416	3.5474	16.5403	16.7107
	-8.4337	-10.1345	-8.7087	-6.8979	-33.9220	-30.0869

= - [E(LUMO) - E(HOMO)]/2; = [E(LUMO) + E(HOMO)]/2; = [E(LUMO) – E(HOMO)]/2; *S* = ˝ = $^2/2$

[a]This work, [b]From Ref [24], [c]From Ref [30], [c]From Ref [30], [c]From Ref [30], [c]From Ref [30],

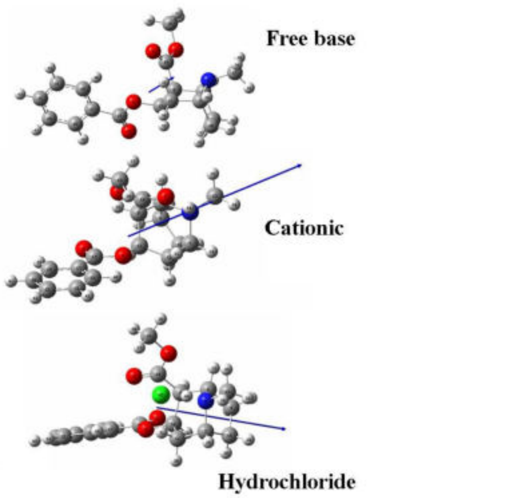

Figure S1. Dipole moment values for the free base, cationic and hydrochloride cocaine species calculated in gas phase at the B3LYP/6-31G* level of theory showing the corresponding magnitudes and orientations of their vectors.

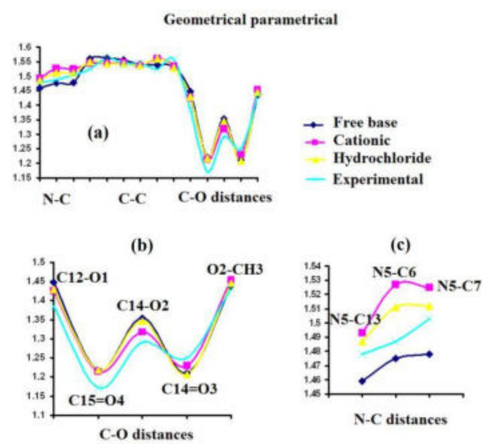

Figure S2. Theoretical geometrical parameters obtained for the free base, cationic and hydrochloride cocaine species calculated in gas phase at the B3LYP/6-31G* level of theory compared with those corresponding to the hydrochloride cocaine in the solid phase [1].

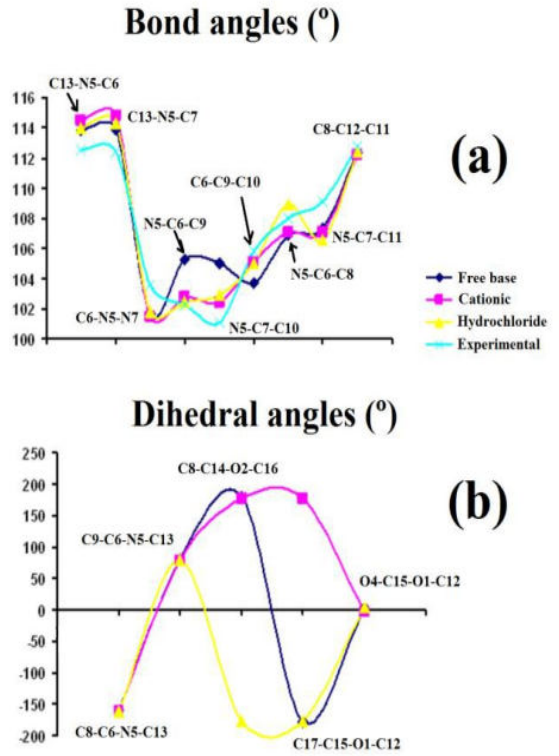

Figure S3. Bond and dihedral angles calculated for the free base, cationic and hydrochloride cocaine species in gas phase at the B3LYP/6-31G* level of theory compared with those corresponding to the hydrochloride cocaine in the solid phase [1].

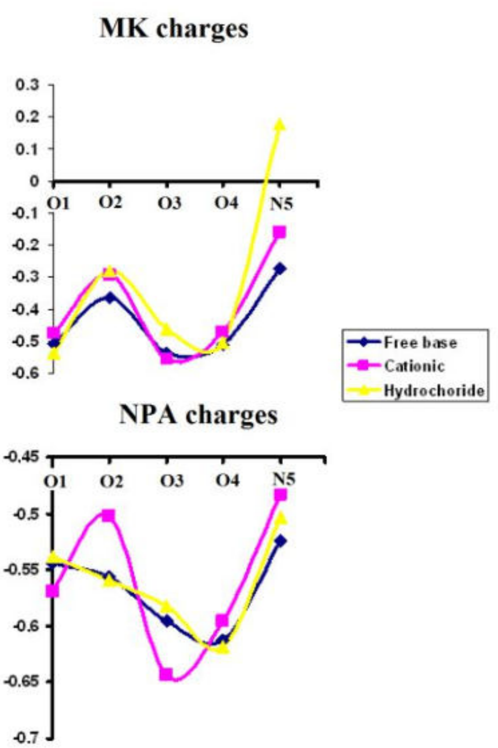

Figure S4. Variations MK (upper) and NPA (bottom) charges on the O and N atoms corresponding to the free base, cationic and hydrochloride cocaine species calculated in gas phase at the B3LYP/6-31G* level of theory.

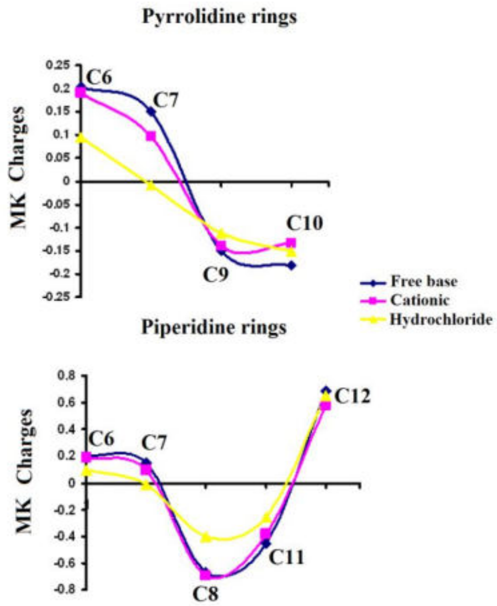

Figure S5. Variations of the MK charges on the C atoms corresponding to the pyrrolidine (upper) and piperidine rings (bottom) of the free base, cationic and hydrochloride cocaine species calculated in gas phase at the B3LYP/6-31G* level of theory.

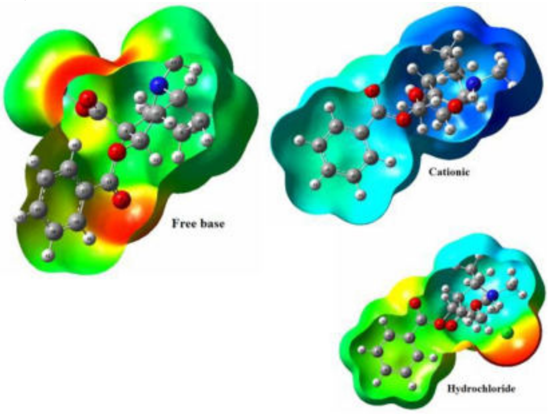

Figure S6. Calculated electrostatic potential surfaces on the molecular surfaces of the free base, cationic and hydrochloride cocaine species in gas phase. Color ranges. In au: from red -0.056 to blue +0.056. B3LYP functional and 6-31G* basis set. Isodensity value of 0.005.

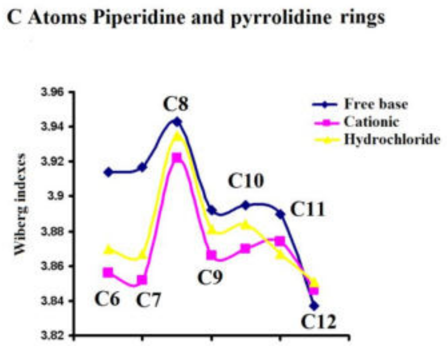

Figure S7. Variations of the bond orders for the C atoms corresponding to the pyrrolidine (C6, C7, C9 and C10) and piperidine (C6, C7, C8, C11 and C12) rings of the free base, cationic and hydrochloride cocaine species calculated in gas phase at the B3LYP/6-31G* level of theory.

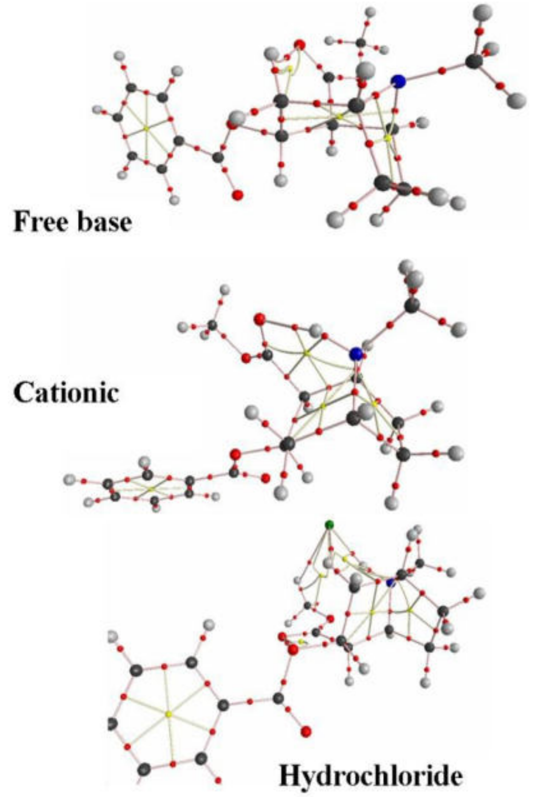

Figure S8. Molecular graphics for the free base, cationic and hydrochloride cocaine species in gas phase showing the geometry of all their bond critical points (BCPs) and ring critical points (RCPs) at the B3LYP/6-31G* level of theory.

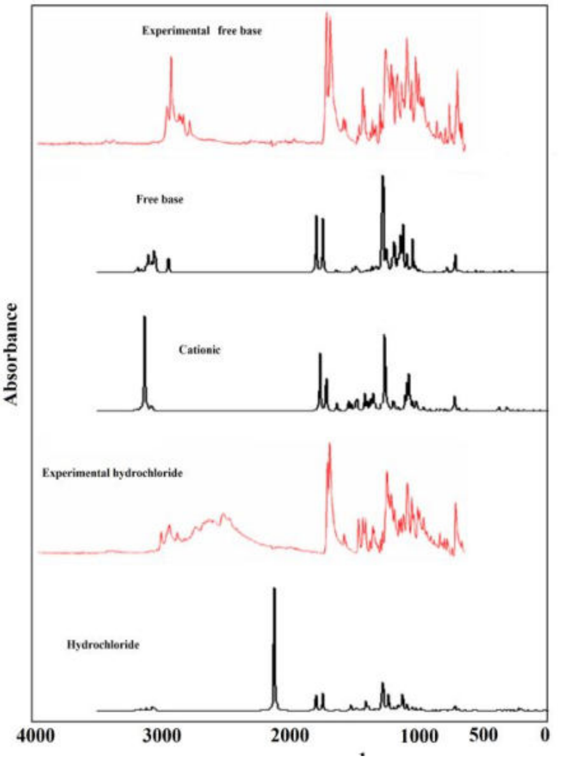

Figure S10. Comparisons between the experimental available Raman spectra of free base and hydrochloride species of cocaine in the solid states [5,63] with the corresponding predicted for the free base, cationic and hydrochloride species in the gas phase at B3LYP/6-311++G** level of theory.

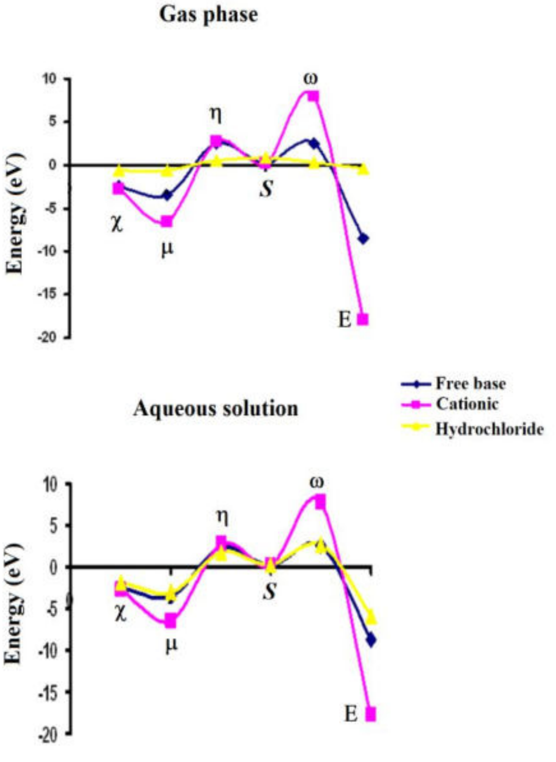

Figure S9. Descriptors calculated for the free base, cationic and hydrochloride cocaine species in gas and aqueous solution phases at the B3LYP/6-31G* level of theory.

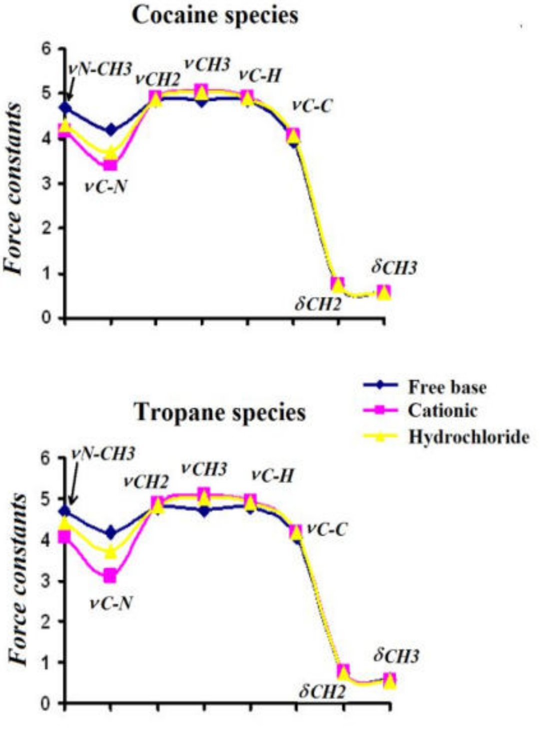

Figure S11. Harmonic force constants calculated for the free base, cationic and hydrochloride cocaine species (upper) compared with those calculated for the corresponding species of tropane alkaloid in gas and aqueous solution phases at the B3LYP/6-31G* level of theory.

REFERENCES:

[1] Gabe, E.J.; Barnes, W.H. (1963), The Crystal and Molecular Structure of Cocaine Hydrochloride, Acta Cryst.. 16, 796-801.

[2] Hrynchuk, R.J.; Barton, R.J.; Robertson, B.E. (1981), The crystal structure of free base cocaine, C17H21NO4, Crystallographic in Biochemistry and pharmacology, Acta Cryst. A37 C72.

[3] Patel, R.C.; Dutta, D.; Schonfeld, S.A. (1987), Free-base cocaine use associated with bronchiolitis obliterans organizing pneumonia, Ann Intern Med. 107(2), 186-187.

[4] Zhu, N.; Reynols, M.; Klein, C.L. (1994), (-) Norcocaine, Acta Cryst. C50, 2067-2069.

[5] Ryder, A.G.; O'Connor, G.M.; Glynn, J.T. (2000), Quantitative analysis of cocaine in solid mixtures using Raman spectroscopy and chemometric methods, Journal of Raman Spectroscopy 31(3), 221-227.

[6] Pan, Y.; Gao, D.; Yang, W.; Cho, H.; Yang, G.; Tai, H-H.; Zhan, C-G. (2005), Computational redesign of human butyrylcholinesterase for anticocaine medication, PNAS, 102(46), 16656–16661.

[7] Zhan, C-G.; Deng, S-X.; Skiba, J.G.; Hayes, B.A.; Tschampel, S.M.; Shields, G.C.; Landry, D.W. (2005), First-principle studies of intermolecular and intramolecular catalysis of protonated cocaine, J Comput Chem. 26(10), 980–986.

[8] Zheng, F.; Yang, W.; Ko, M-C.; Liu, J.; Cho, H.; Gao, D.; Tong, M.; Tai, H-H.; Woods, J.H.; Zhan, C-G. (2008), Most Efficient Cocaine Hydrolase Designed by Virtual Screening of Transition States, J Am Chem Soc. 130(36), 12148–12155.

[9] Davies, A.G.; Burnett, A.D.; Fan, W.; Linfield, E.H.; Cunningham, J.E. (2008), Terahertz spectroscopy of explosives and drugs, Materials Today, 11(3), 18-26.

[10] Maharaj, R. (2008), Quantitative Analysis Of Cocaine Using Fourier Transform Infra Red Spectroscopy-Attenuated Total Reflectance: A Preliminary Investigation, The Internet Journal of Third World Medicine, 7(2), 1-5.

[11] Distinguishing Cocaine HCl from Cocaine Base by FTIR, Copyright 2009, Spectros Associateswww.Spectros1.com.

[12] Rodrigues, N.V.S.; Cardoso, E.M.; Andrade, M.V.O.; Donnicia, C.L.; Sena, M.M. (2013), Analysis of Seized Cocaine Samples by using Chemometric Methods and FTIR Spectroscopy, J. Braz. Chem. Soc. 24(3), 507-517.

[13] Babu, N.S.; Tadesse, S. (2015), Computational studies on molecular structure and interpretation of vibrational spectra, thermodynamical and HOMO-LUMO analysis of mephedrone using density functional theory and ab initio methods, European Journal of Biomedical & Pharmaceutical sciences, 2(2), 18-33.

[14] Penido, C.A.; Pacheco, M.T.; Zângaro, R.A.; Silveira L. Jr., (2015), Identification of different forms of cocaine and substances used in adulteration using near-infrared Raman spectroscopy and infrared absorption spectroscopy, J Forensic Sci. 60(1), 171-178.

[15] Singh Bumbrah, G.; Sharma, R.M. (2016), Raman spectroscopy – Basic principle, instrumentation and selected applications for the characterization of drugs of abuse, Egyptian Journal of Forensic Sciences 6, 209-215

[16] Guha, P.; Harraz, M.M.; Snyder, S.H. (2016), Cocaine elicits autophagic cytotoxicity via a nitricoxide-GAPDH signaling cascade, PNAS, 113(5), 1417–1422.

[17] Buckett, W.R.; Haining, C.G. (1965), Some pharmacological studies on the optically active isomers of hyoscine and hyoscyamine, Brit. J. Pharmacol. 24, 138-146.

[18] Cantor, E.H.; Abraham, S; Marcum, E.A.; Spector, S. (1983), Structure-activity requirements for hypotension and et-adrenergic receptor blockade by analogues of atropine, European Journal of Pharmacology, 90, 75-83.

[19] Hammon, K.; DeMartino, B. (1985), Postoperative Delirium Secondary to Atropine Premedication, Anesthesia Progress 107-108.

[20] Armstrong, D.W.; Han, S.M.; Han, Y.I. (1987), Separation of Optical Isomers of Scopolamine, Cocaine, Homatropine, and Atropine, Analytical Biochemistry 167, 261-264.

[21] Niu, Y-Y; Yang, L-M; Liu, H-Z; Cui, Y-Y; Zhu, L; Feng, J-M; Yao, J-H; Chen, H-Z; Fan, B-T; Chen, Z-N; Lu, Y. (2005), Activity and QSAR study of baogongteng A and its derivatives as muscarinic agonists, Bioorganic & Medicinal Chemistry Letters 15, 4814–4818.

[22] Xiang, X-H; Wang, H-L; Wu, W-R; Guo, Y.; Cao, D-Y.; Wang, H-S.; Zhao, Y. (2006), Ethological analysis of scopolamine treatment or pretreatment in morphine dependent rats, Physiology & Behavior 88, 183–190.

[23] De Simone, R.; Margarucci, L.; De Feo, V. (2008) Tropane alkaloids: An overview, Pharmacologyonline 1, 70-89.

[24] Beyer, J.; Drummer, O.H.; Maurer, H.H. (2009), Analysis of toxic alkaloids in body samples, Forensic Science International 185, 1–9.

[25] Klinkenberg, I.; Blokland, A. (2010), The validity of scopolamine as a pharmacological model for cognitive impairment: A review of animal behavioral studies, Neuroscience and Biobehavioral Reviews 34, 1307–1350.

[26] Wang, J-H.; Chena, Y-M.; Carlson, S.; Li, L.; Hu, X-T.; Ma, Y-Y. (2012), Interactive effects of morphine and scopolamine, MK-801, propanolol on spatial working memory in rhesus monkeys, Neuroscience Letters 523, 119– 124.

[27] Veeranjaneyulu, P.; Rao, T.B.; Mantha, S.; Vaidyanathan, G. A sensitive method for the estimation of scopolamine um human plasma using ACQUITY UPLC and Xevo TQ-S, Waters Corporation, Bangalore, India, 1-7 (2012).

[28] Sweta, V.R.; Lakshmi, T. (2015), Pharmacological profile of tropane alkaloids, Journal of Chemical and Pharmaceutical Research, 7(5), 117-119.

[29] Fernandes de Oliveira Penido, C.A.; Silveira Jr., L.; Tavares Pacheco, M.T. (2012), Quantification of binary mixtures of cocaine and adulterants using dispersive Raman and FTIR spectroscopy and principal component regression, Instrumentation Science & Technology, 40(5)

[30] Cameron, D.G.; Kauppinen, J.K.; Moffatt, D.J.; Mantsch, H.H. (1982), Precision in Condensed Phase, Vibrational Spectroscopy, Appl. Spectrosc. 36(3), 245-250.

[31] Mainali, D.; Seelenbinder, J. (2016), Automated fast screening test method for cocaine identification in seized drug samples using portable Fourier transform infrared (FT-IR) instrument, Appl Spectrosc., 70(5), 916-922.

[32] Rudyk, R.; Brandán, S.A. (2017), Vibrational assignment of alkaloid tropane hydrochloride by using their infrared spectrum, internal coordinates and the SQM procedure, Paripex Indian Journal of Reasearch 6(8), 616-623.

[33] Lazny, R. Ratkiewicz, A. Nodzewska, A. A. Wynimko, L. Siergiejczyk, Determination of the N-methyl stereochemistry in tropane and granatane derivatives in solution: a computational and NMR spectroscopic study, Tetrahedron Letters, (2012).

[34] Becke, A.D. (1988), Density-functional exchange-energy approximation with correct asymptotic behavior, Phys. Rev. A38, 3098-3100.

[35] Lee, C.; Yang, W.; Parr. R.G. (1988), Development of the Colle-Salvetti correlation-energy formula into a functional of the electron density, Phys. Rev. B37, 785-789.

[36] Pauling, P.; Datta, N. (1980), Anticholinergic substances: A single consistent conformation, Proc. Natl. Acad. Sci. 77(2), 708-712.

[37] Parr, R.G.; Pearson, R.G. (1983), Absolute hardness: companion parameter to absolute electronegativity, J. Am. Chem. Soc. 105, 7512-7516.

[38] Brédas, J-L (2014), Mind the gap!, Materials Horizons 1, 17–19.

[39] Romani, D.; Tsuchiya, S.; Yotsu-Yamashita, M.; Brandán, S.A. (2016), Spectroscopic and structural investigation on intermediates species structurally associated to the tricyclic bisguanidine compound and to the toxic agent, saxitoxin, J. Mol. Struct. 1119, 25-38.

[40] Romani, D.; Márquez, M.J.; Márquez, M.B.; Brandán, S.A. (2015), Structural, topological and vibrational properties of an isothiazole derivatives series with antiviral activities, J. Mol. Struct. 1100, 279-289.

[41] Chain, F.; Iramain, M.A.; Grau, A.; Catalán, C.A.N.; Brandán, S.A. (2016), Evaluation of the structural, electronic, topological and vibrational properties of N-(3,4-dimethoxybenzyl)-hexadecanamide isolated from Maca (Lepidium meyenii) using different spectroscopic techniques, J. Mol. Struct. 1119, 25-38.

[42] Nielsen, A.B.; Holder, A.J. Gauss View 3.0, User's Reference, GAUSSIAN Inc., Pittsburgh, PA, 2000–2003.

[43] Frisch, M.J. et al., GAUSSIAN 09, Revision A.02, Gaussian, Inc., Wallingford, CT, 2009.

[44] Gyermek, L. The role of the tropane skeleton in drug research, was presented as a lecture in Hungarian, on the occasion of his election as Foreign Member of the Hungarian Academy of Medical Sciences (Division V-Medical Sciences), September, (2005).

[45] Hamor, T.A.; Kings, N. (1980), Structure of 3□-Bromotropane Hydrobromide Monohydrate, Acta Cryst.. B36, 3153-3155.

[46] Bode, J.; Stam, C. H. (1982), The Absolute Configuration of the Tropane Alkaloid 6□,7□-Epoxy-l□H,5□H~tropan-3□-yl(-)-2,3-Dihydroxy-2-phenylpropionate from its n-Butylbromide, Acta Cryst.. B38, 333-335.

[47] Muńoz, M.A.; Muńoz, O.; Joseph-Nathan, P. (2010), Absolute Configuration Determination and Conformational Analysis of (2)-(3S,6S)-3a,6b-Diacetoxytropane Using Vibrational Circular Dichroism and DFT Techniques, Chirality 22, 234–241.

[48] Miertus, S.; Scrocco, E.; Tomasi, J. (1981), Electrostatic interaction of a solute with a continuum. Chem. Phys. 55, 117–129.

[49] Tomasi, J.; Persico, J. (1994), Molecular Interactions in Solution: An Overview of Methods Based on Continous Distributions of the Solvent, Chem. Rev. 94, 2027-2094.

[50] Marenich, A.V.; Cramer, C.J.; Truhlar, D.G. Universal solvation model based on solute electron density and a continuum model of the solvent defined by the bulk dielectric constant and atomic surface tensions, J. Phys. Chem. B113 (2009) 6378-6396.

[51] Ugliengo, P. MOLDRAW Program, University of Torino, Dipartimento Chimica IFM, Torino, Italy, 1998.

[52] a) Rauhut, G.; Pulay, P. (1995), J. Phys. Chem. 99 (1995) 3093-3099. b) Correction: G. Rauhut, P. Pulay, J. Phys. Chem. 99 14572.

[53] Sundius, T. (2002), Scaling of ab initio force fields by MOLVIB, Vib. Spectrosc. 29, 89-95.

[54] Besler, B.H.; Merz Jr, K.M.; Kollman, P.A. (1990), Atomic charges derived from demiempirical methods, J. Comp. Chem. 11, 431-439.

[55] Glendening, E.D.; Badenhoop, J.K.; Reed, A.D.; Carpenter, J.E.; Weinhold, F. NBO 3.1; Theoretical Chemistry Institute, University of Wisconsin; Madison, WI, 1996.

[56] Biegler-Köning, F.; Schönbohm, J.; Bayles, D. (2001), AIM2000; A Program to Analyze and Visualize Atoms in Molecules, J. Comput. Chem. 22, 545.

[57] Bader, R.F.W. Atoms in Molecules, A Quantum Theory, Oxford University Press, Oxford, 1990, ISBN: 0198558651.

[58] Bushmarinov, I.S.; Lyssenko, K.A.; Antipin, M.; Yu (2009), Atomic energy in the Atoms in Molecules theory and its use for solving chemical problems, Russian Chem. Rev. 78(4), 283-302.

[59] Romani, D.; Brandán, S.A. (2015), Effect of the side chain on the properties from cidofovir to brincidofovir, an experimental antiviral drug against to Ebola virus disease, Arabian Journal of Chemistry http://dx.doi.org/10.1016/j.arabjc.2015.06.030.

[60] Romani, D.; Brandán, S.A. (2015), Structural, electronic and vibrational studies of two 1,3-benzothiazole tautomers with potential antimicrobial activity in aqueous and organic solvents. Prediction of their reactivities, Computational and Theoretical Chem., 1061, 89-99.

[61] Singh, S. (2000), Chemistry, Design, and Structure-Activity Relationship of Cocaine Antagonists, Chem. Rev. 100, 925-1024.

[62] http://webbook.nist.gov/cgi/cbook.cgi?ID=C50362&Mask=80#IR-Spec

[63] Fedchak, (2014), S. Presumptive Field Testing Using Portable Raman Spectroscopy, Las Vegas Metropolitan Police Department, Award Number 2010-DN-BX-K201.

[64] Keresztury, G.; Holly, S.; Besenyei, G.; Varga, J.; Wang, A.Y.; Durig, J.R. (1993), Vibrational spectra of monothiocarbamates-II. IR and Raman spectra, vibrational assignment, conformational analysis and ab initio calculations of S-methyl-N,N-dimethylthiocarbamate Spectrochim. Acta, 49A, 2007-2026.

[65] Michalska, D.; Wysokinski, R. (2005), The prediction of Raman spectra of platinum(II) anticancer drugs by density functional theory, Chemical Physics Letters, 403, 211-217.

[66] Romano, E.; Davies, L.; Brandán, S.A. (2017), Structural properties and FTIR-Raman spectra of the anti-hypertensive clonidine hydrochloride agent and their dimeric species, J. Mol. Struct. 1133, 226-235.

[67] Chain, F.E.; Ladetto, M.F.; Grau, A.; Catalán, C.A.N.; Brandán, S.A. (2016), Structural, electronic, topological and vibrational properties of a series of N-benzylamides derived from Maca (Lepidium meyenii) combining spectroscopic studies with ONION calculations, J. Mol. Struct. 1105, 403-414.

[68] Márquez, M.J.; Márquez, M.B.; Cataldo, P.G.; Brandán, S.A. (2015), A Comparative Study on the Structural and Vibrational Properties of Two Potential Antimicrobial and Anticancer Cyanopyridine Derivatives, Open Journal of Synthesis Theory and Applications, 4, 1-19.

[69] Márquez, M.B.; Brandán, S.A. (2014), A Structural and Vibrational Investigation on the Antiviral Deoxyribonucleoside Thymidine Agent in Gas and Aqueous Solution Phases, Int. J. Quantum Chem. 114, 209-221.

[70] Cataldo, P.G.; Castillo, M.V.; Brandán, S.A. (2014), Quantum Mechanical Modeling of Fluoromethylated-pyrrol Derivatives a Study on their Reactivities, Structures and Vibrational Properties, J Phys Chem Biophys, 4(1), 4-9.

[71] Brizuela, A.B.; Raschi, A.B.; Castillo, M.V.; Leyton, P.; Romano, E.; Brandán, S.A. (2013), Theoretical structural and vibrational properties of the artificial sweetener sucralose, Comp. Theor. Chem. 1008, 52–60.